SAND2023-01311C

Sandia National Laboratories

A framework for experimental data-driven assessment of Magnetized Liner Inertial Fusion stagnation image metrics

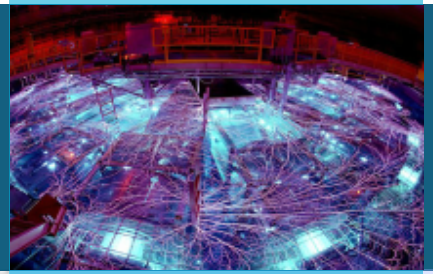

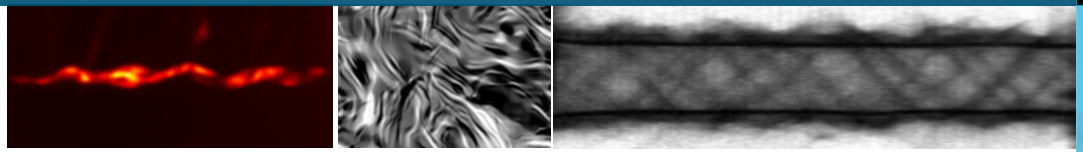

PRESENTED BY

William Lewis

ICDDPS-4
4/19/23

Collaborators: Eric Harding, David Yager-Elorriaga, Jeffrey Fein, Patrick Knapp, Kristian Beckwith, and David Ampleford

ks to the entire AMPRD and MagLIF teams for useful

Sandia National Laboratories is a multimission laboratory managed and operated by National Technology & Engineering Solutions of Sandia, LLC, a wholly owned subsidiary of Honeywell International Inc., for the U.S. Department of Energy's National Nuclear Security Administration under contract DE-NA0003525.

Sandia National Laboratories is a multimission laboratory managed and operated by National Technology and Engineering Solutions of Sandia LLC, a wholly owned subsidiary of Honeywell International Inc. for the U.S. Department of Energy's National Nuclear Security Administration under contract DE-NA0003525.

physics systems and applications ripe for data-driven approaches.

Tracking blobs in fusion plasmas at the Tokamak à Configuration Variable

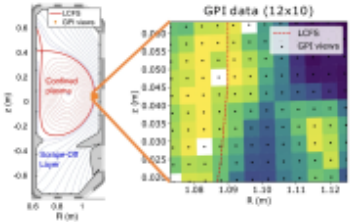

W. Han *et al.* Scientific Reports **12**, (2022)

Classification of Caltech Spheromak image data

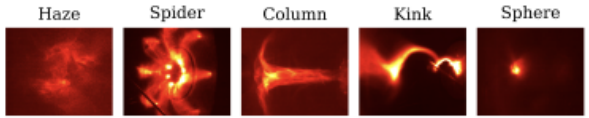

M.J. Falato *et al.* J. Plasma Phys. **88**, 895880603 (2022)

Characterizing instability growth in magneto-inertial fusion

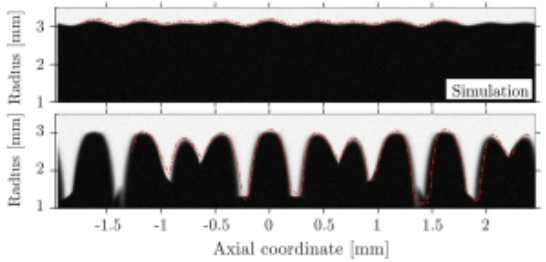

D.E Ruiz *et al.* Phys. Rev. Lett. **128**, 255001 (2022).

Automation and control of laser wakefield accelerators

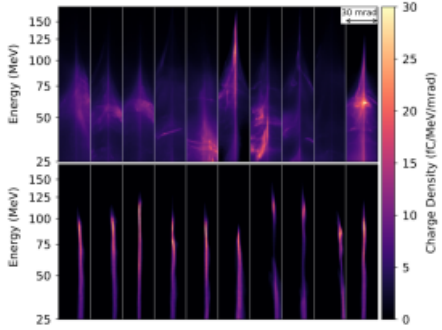

R.J. Shalloo *et al.* Nat. Comm. **11**, 6355 (2020).

Image enhancement of helioseismic and magnetic imager data

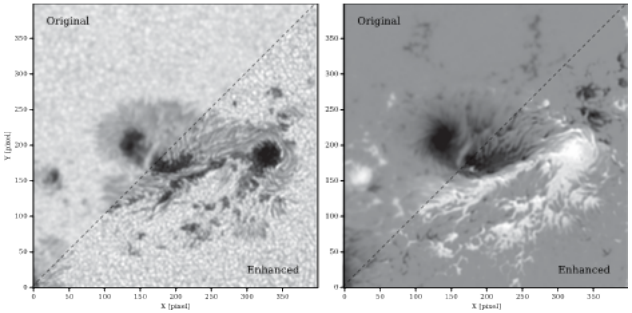

C.J. Díaz Baso and A. Aensio Ramos A &A. **614**, A5 (2018).

Sparse view tomographic reconstruction

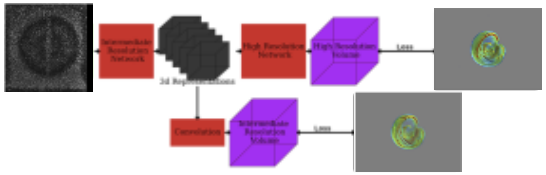

B.T. Wolfe *et al.* Rev. Sci. Instrum. **94**, 023504 (2023).

physics systems and applications ripe for data-driven approaches.

Segmentation convolutional neural network enabled reproducible and automated workflows

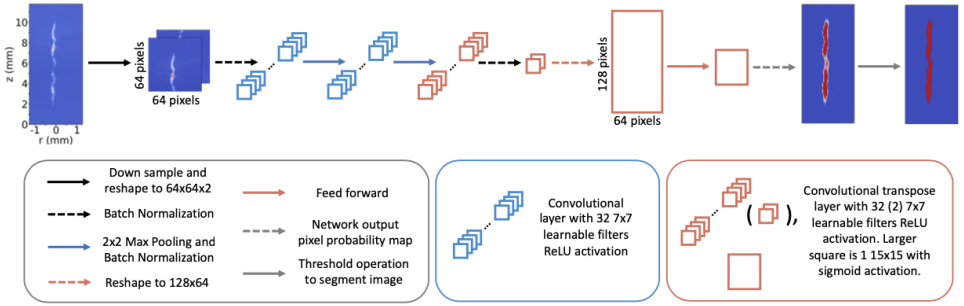

Statistical characterization of slowly varying background, noise, and signal levels

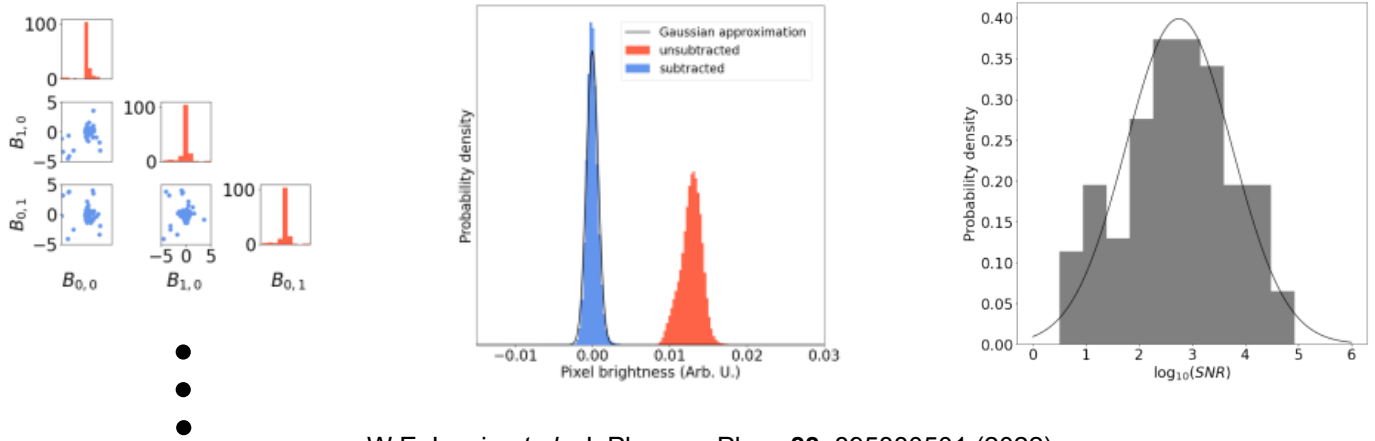

W.E. Lewis *et al.*, J. Plasmas Phys. **88**, 895880501 (2022).

physics systems and applications ripe for data-driven approaches.

Segmentation convolutional neural network enabled reproducible and automated workflows

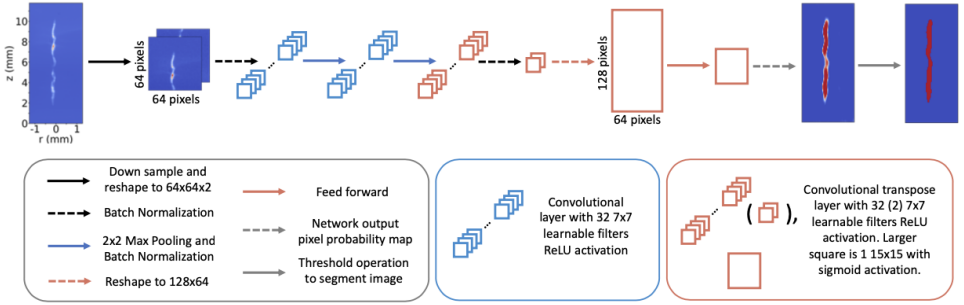

Apart from being a shameless plug, this effort enabled the results I'm presenting today.

W.E. Lewis *et al.*, J. Plasmas Phys. **88**, 895880501 (2022).

can contribute to understanding performance and reproducibility.

- Magnetized Liner Inertial Fusion (MagLIF) stagnation images show significant variance arising from
  - variation in a large number of experimental input conditions
  - different spherical crystal x-ray imager configurations

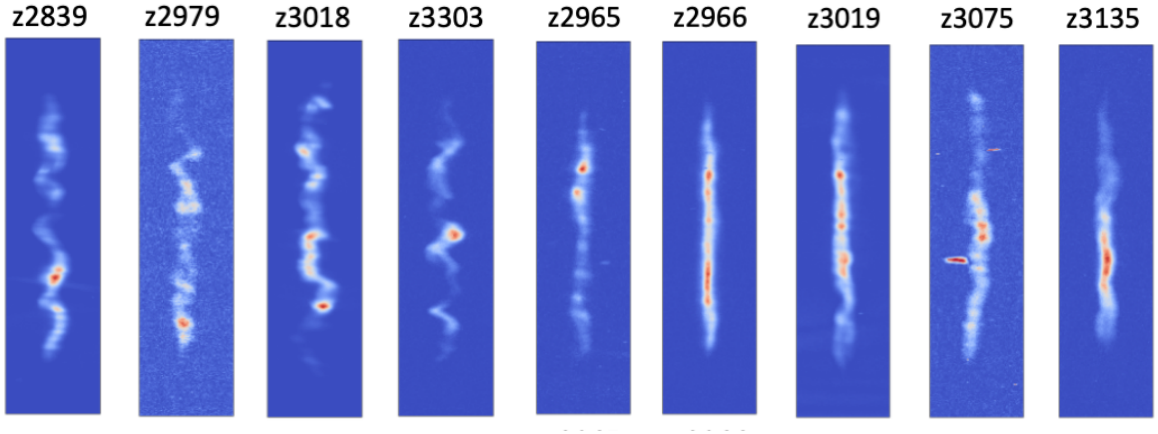

- Need ***meaningful*** metrics to build understanding
  - sensitivities to realities of experiment
    - (e.g. signal-to-noise, registration, imager configuration)
  - physics basis *i.e.* interpretable and/or statistically insightful

can contribute to understanding performance and reproducibility.

- **This talk:**
  - Combine ideas of **data-augmentation** and **experimental data** to understand sensitivities
    - model-free with a small

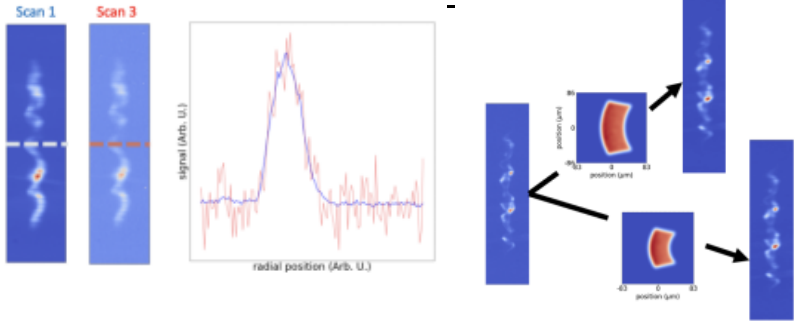

  - Use space-scale representation to classify images

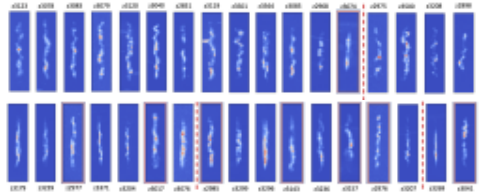

random	u	c
$\tilde{u}$	0.74 ± 0.06	0.74 ± 0.11
$\tilde{c}$	0.26 ± 0.06	0.26 ± 0.11

MST	u	c
$\tilde{u}$	0.84	0.47
$\tilde{c}$	0.16	0.53

  - Compare hand-picked to "less intuitive" representati

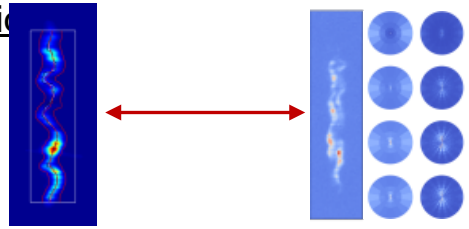

- Need ***meaningful*** metrics to build understanding
  - sensitivities to realities of experiment
    - (e.g. signal-to-noise, registration, imager configuration)
  - physics basis *i.e.* interpretable and/or statistically insightful

can contribute to understanding performance and reproducibility.

- **This talk:**
  - Combine ideas of **data-augmentation** and **experimental data** to understand sensitivities
    - model-free with a small

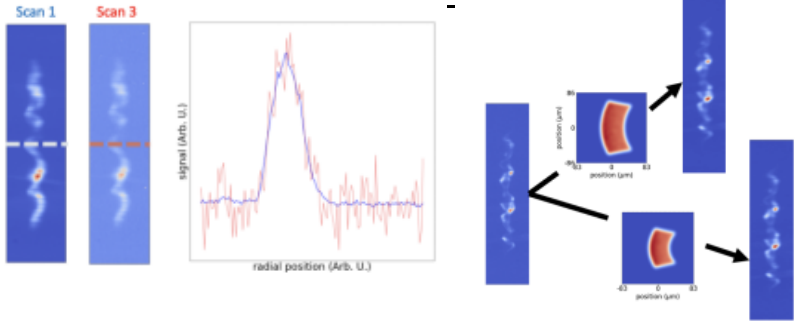

  - Use space-scale representation to classify images

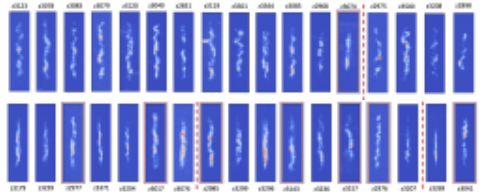

random	u	c
$\tilde{u}$	0.74 ± 0.06	0.74 ± 0.11
$\tilde{c}$	0.26 ± 0.06	0.26 ± 0.11

MST	u	c
$\tilde{u}$	0.84	0.47
$\tilde{c}$	0.16	0.53

  - Compare hand-picked to "less intuitive" representati

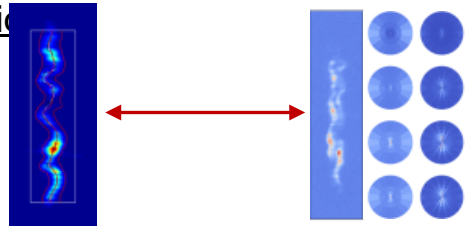

- Need ***meaningful*** metrics to build understanding
  - sensitivities to realities of experiment
    - (e.g. signal-to-noise, registration, imager configuration)
  - physics basis *i.e.* interpretable and/or statistically insightful

But first things "first", where do these images come from?!
A.K.A the plasma science in ICDD**PS**-4

Sandia's Z Pulsed Power Facility

The Earth's largest pulsed power machine

Sandia's Z Pulsed Power Facility

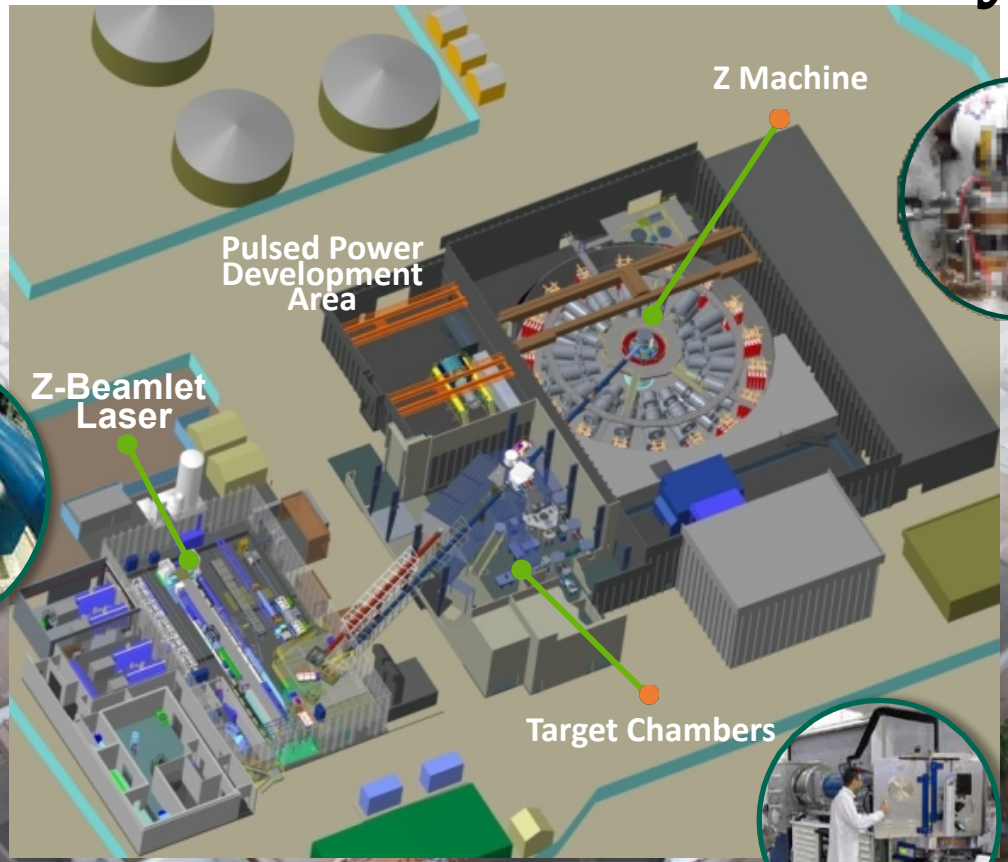

Capabilities

- >20 MA peak current
- 4 kJ, 1 TW laser
- kJ's warm x-rays
- kJ's fusion yield
- Mbar's planar drive
- >2MJ's soft x-rays.

fielded on Z relies on three stages to reach fusion relevant conditions.

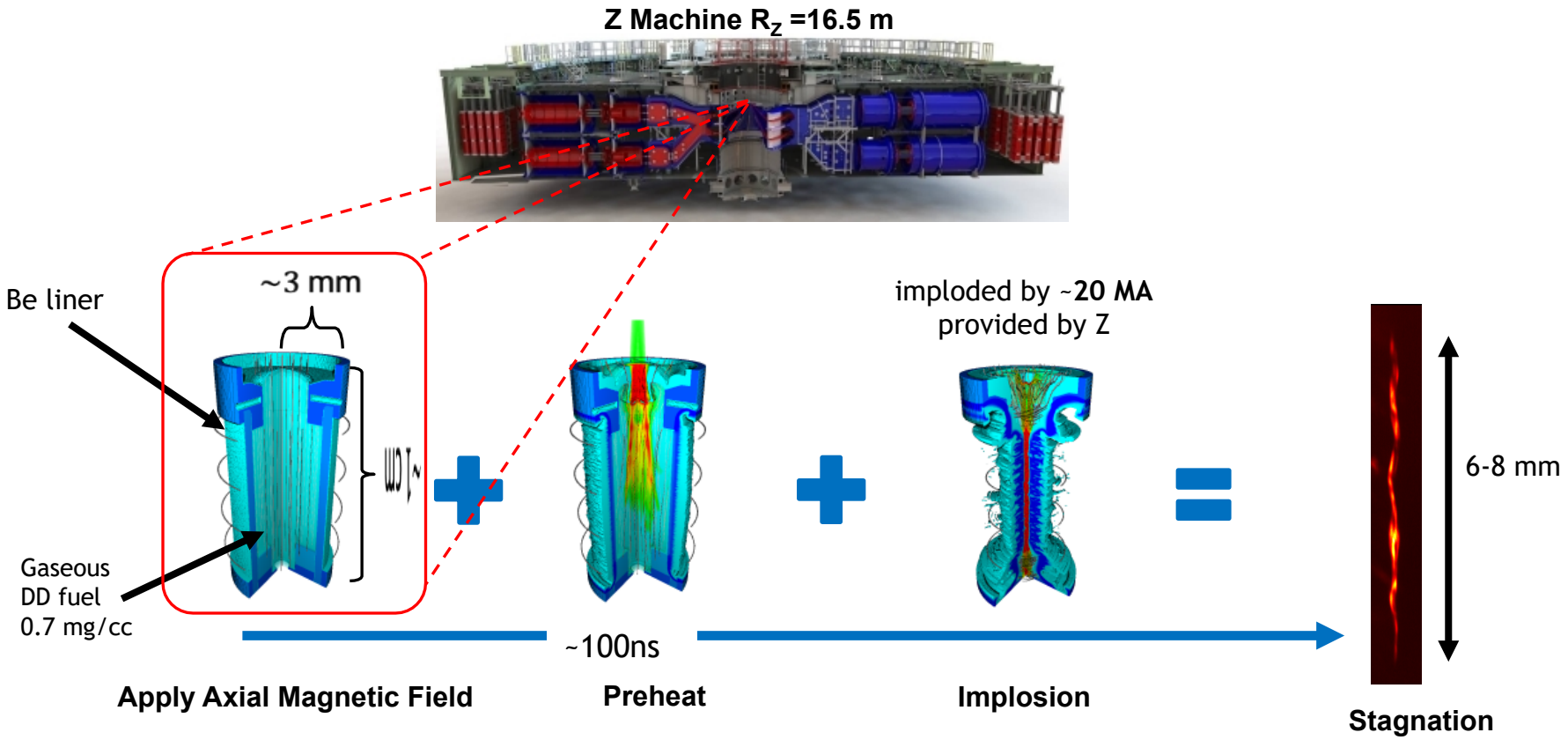

S.A. Slutz *et. al.*, Phys. Plasmas **17**, 056303 (2010).
M.R. Gomez *et al.* Phys. Rev. Lett. **113**, 155003 (2014).

Helmholtz-like coils are used to premagnetize the MagLIF load

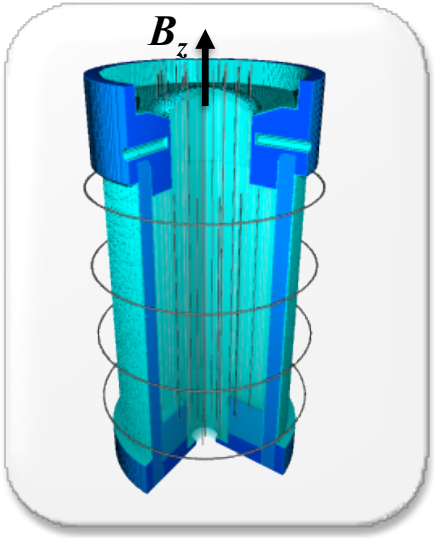

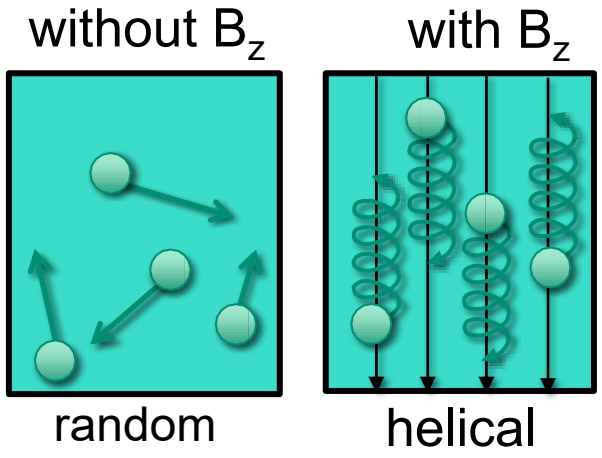

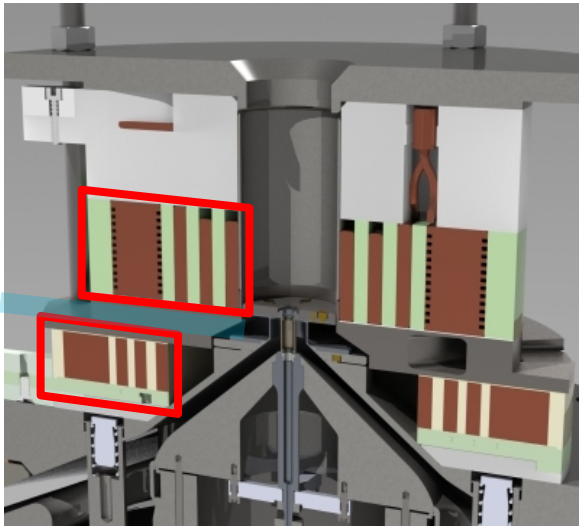

Premagnetize fuel

- embed 7-20 T in ~ms timescale
- reduce radial thermal conduction
- compress + traps fusion products

D. C. Rovang *et al.*, Rev. Sci. Instrum. **85**, 124701 (2014).

Z-Beamlet laser preheats the fuel establishing a higher adiabat

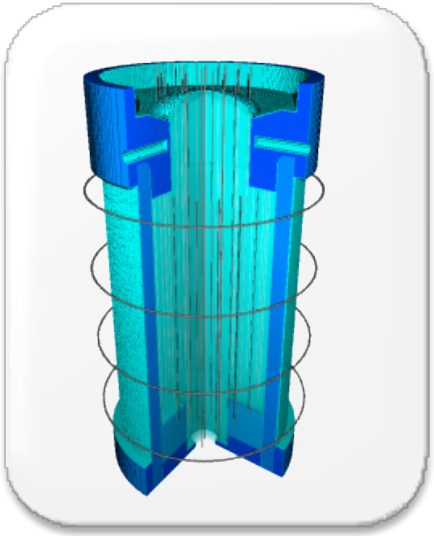

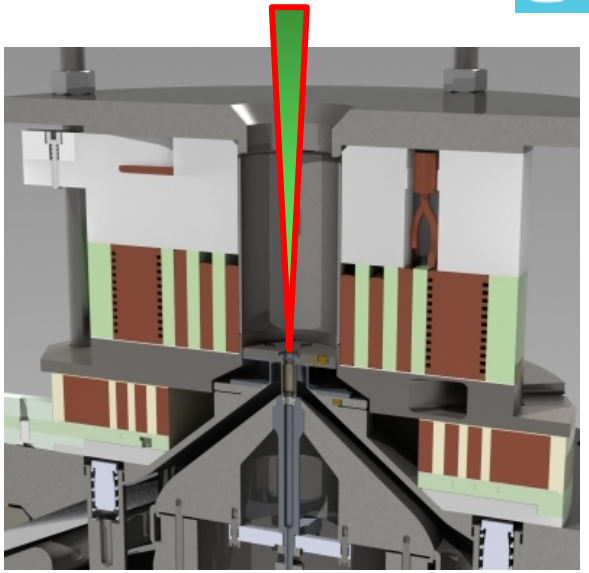

Preheat the fuel

- Z-Beamlet laser delivers ~2-3 kJ to the Z chamber.
- Laser heats fuel through Inverse Bremsstrahlung (~100-200 eV, 1-2 kJ)
- Laser preheat sets the adiabat of the implosion.

M. R. Weis, *et al.*, Phys. Plasmas **28,** 012705 (2021).
A. J. Harvey-Thompson, *et al.*, Phys. Plasmas **27,** 113301 (2020).
A. J. Harvey-Thompson, *et al.*, Phys. Plasmas **26**, 032707 (2019).
A. J. Harvey-Thompson, *et al.*, Phys. Plasmas **25**, 112705 (2018).
M. Geissel, *et al.*, Phys. Plasmas **25**, 022706 (2018).
A. J. Harvey-Thompson, *et al.*, Phys. Rev. E **94**, 051201 (2016).
A. J. Harvey-Thompson, *et al.*, Phys. Plasmas **22**, 122708 (2015).

magnetic pressure driving the liner to implode compressing the fuel

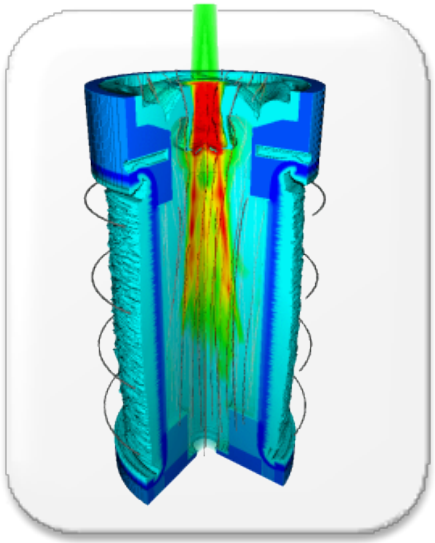

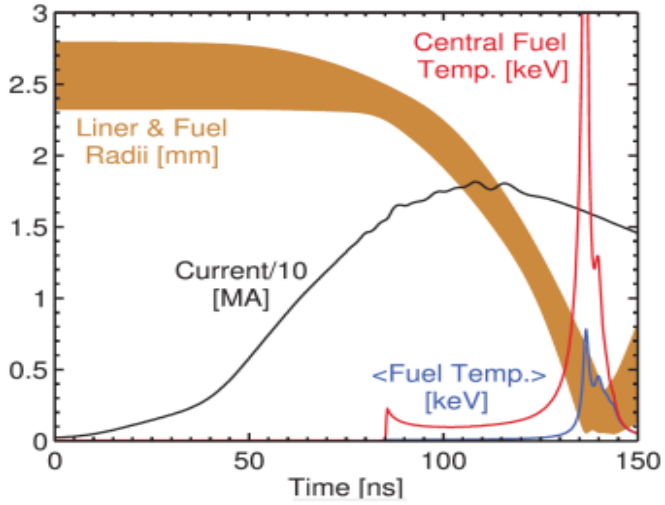

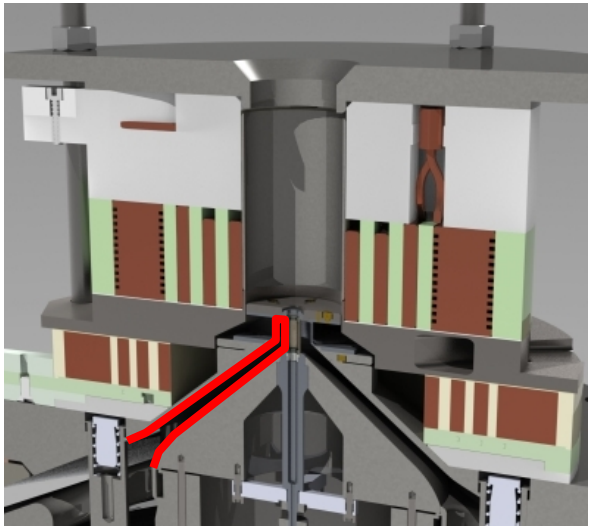

Compress liner and fuel

- Lorentz force accelerated the liner.
- Fuel is then quasi-adiabatically compressed.
- Liner implosion leads to flux compression, amplifying B-field

R. McBride et al., Phys. Plasmas **23**, 012705 (2016).
3D implosion movie courtesy of C. Jennings.

When thermal pressure exceeds magnetic pressure, the liner decelerates resulting in stagnation

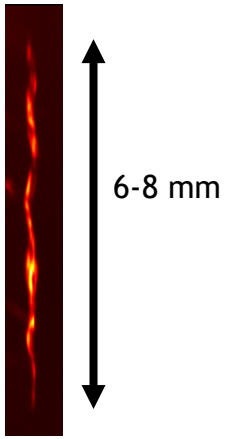

Stagnation

Plasma parameter	Shot z3289
$\dot{R}_{max}$	70 km/s
R_{burn}	50 um
T_{burn}	2.7 keV
p_{burn}	1.9 Gbar
BR	0.2-0.5 MG·cm
τ_{bw}	2 ns
Y (DT equivalent)	2 kJ

S.A. Slutz *et. al.*, Phys. Plasmas **17**, 056303 (2010).
M.R. Gomez *et al.* Phys. Rev. Lett. **113**, 155003 (2014).

MagLIF offers a rich physics platform with paths to high yield at a next generation pulsed power (NGPP) facility.

- Physics:
  - magnetized HED plasmas
  - fusion relevant temperatures and densities
  - thermonuclear neutron generation
- May provide route to fusion-energy on the grid*
  - high-yield pulsed-power ICF has relevant gain factor
    - need G~100

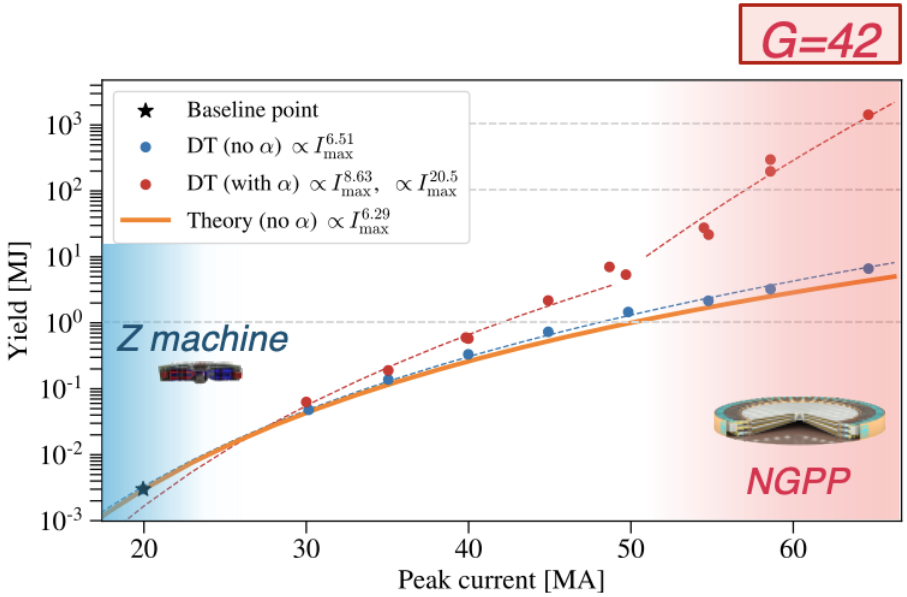

D.E. Ruiz *et. al.*, (Submitted) Phys. Plasmas.

*S. Atzeni and J. Meyer-ter Vehn, *The Physics of Inertial Fusion*, (Oxford University Press Inc., New York, 2009).

we understand and characterize the physics of MagLIF on Z today.

Experimental input conditions

Preheat energy deposited ~0.7 – 1.4 kJ

$B_{z,0}$ ~ 10 – 30 T

Final feed

Laser conditioning

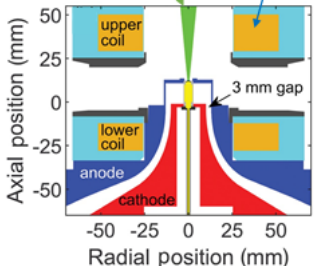

LEH foil thickness

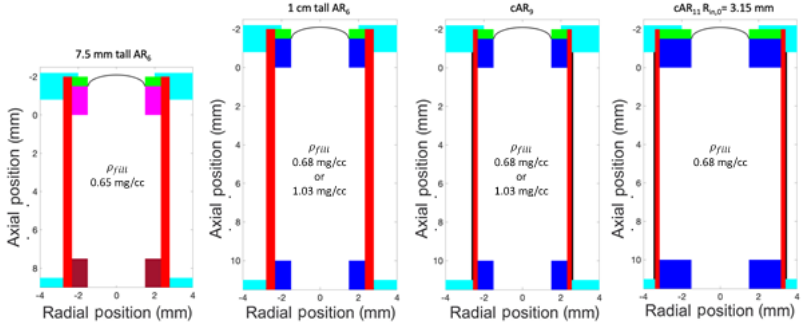

A.J. Harvey-Thompson *et al.* Phys. Plasmas **25**, 112705 (2018).
D.A. Yager-Elorriaga *et al.* Nucl. Fusion **62**, 042015 (2022).
W.E. Lewis *et al.* Phys. Plasmas (Submitted).

Experimental performance

$$\chi = \frac{2}{3}\frac{f_D f_T}{(1+\langle Z\rangle)^2}\frac{\varepsilon_\alpha \tau_E}{V_{HS}}\int_V P_{HS}\frac{\langle \sigma v\rangle_{DT}}{T^2}\,dV$$

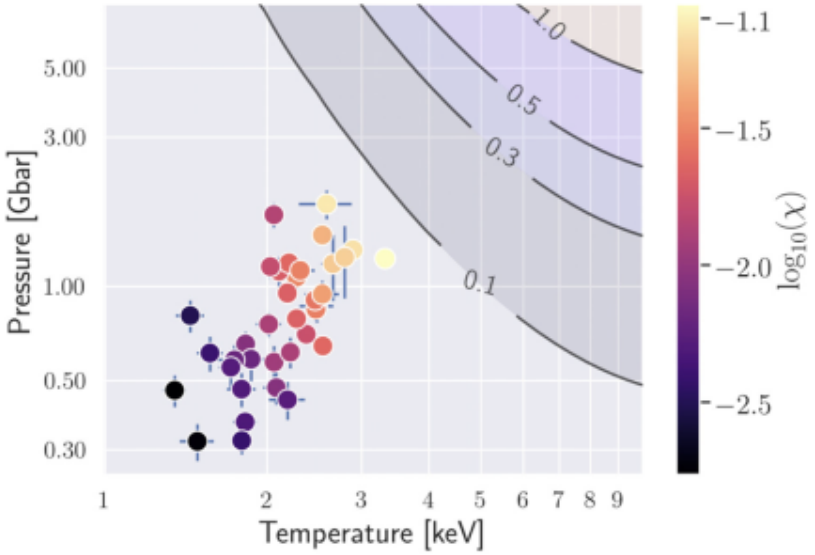

P.F. Knapp *et al.*, Phys. Plasmas **29**, 052711 (2022).

Data-driven methods paired with physics insight, theory, and simulation are playing a key role in this effort.

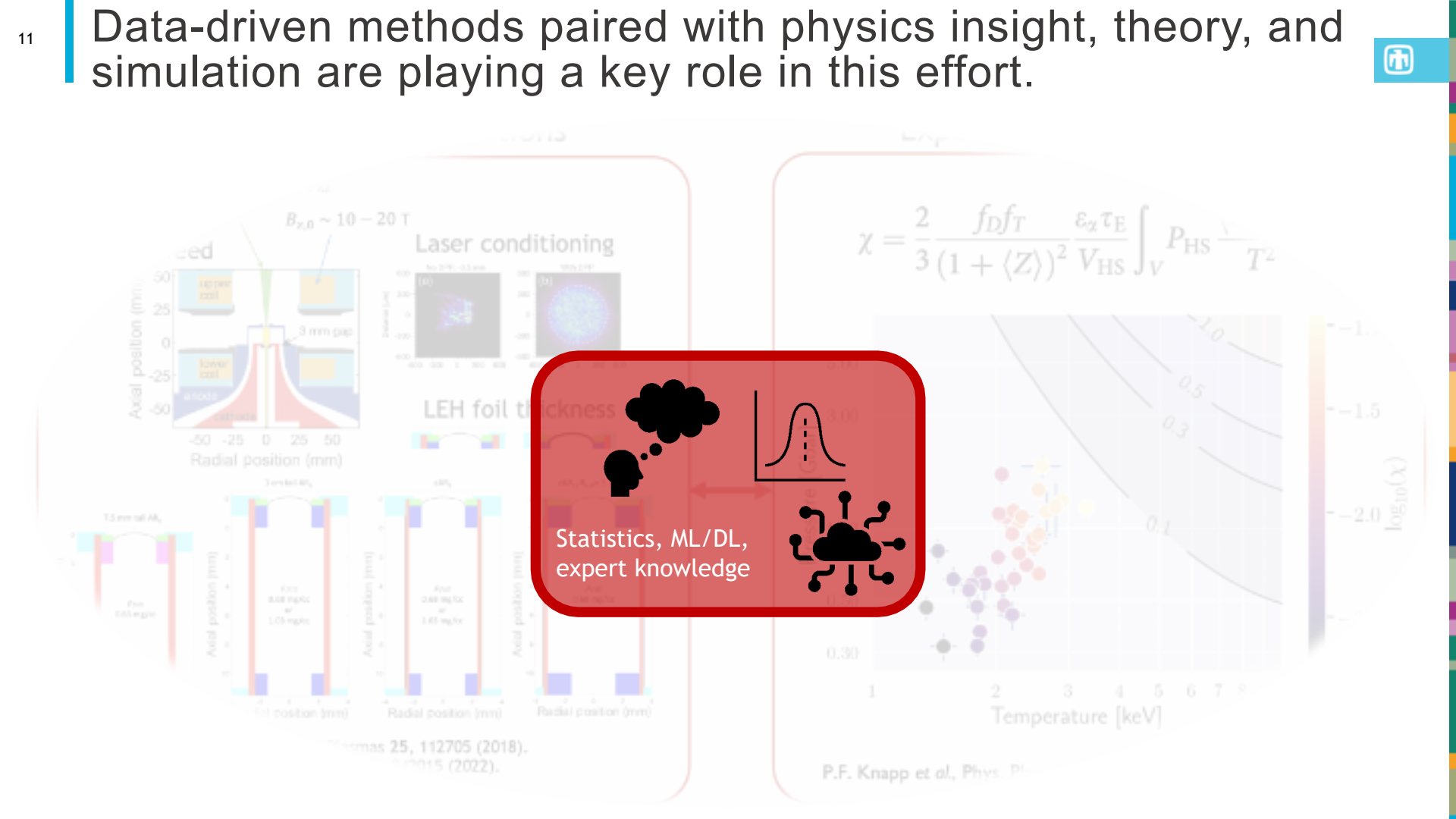

difficult.

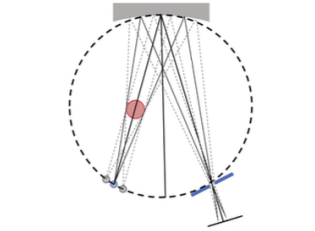

Imager	Configuration	Resolution [μm^2]
Argon Imager(Ar-Imager)	single	15 × 85
Continuum X-ray Imager (CXI)	single	59 × 83
High Resolution Continuum X-ray (CXI)	single	15 × 16
Dual Continuum X-ray (DCXI)	dual	Ch1 54 × 120 Ch2 46 × 84
Iron K-α_1 (IKA1)	dual	Ch1 79 × 82 Ch2 64 × 66
Iron Helium-β (IHEB)	dual	Ch1 63 × 66 Ch2 50 × 53
Cobalt He-w (CHEWI)	dual/orthogonal	Ch1 61 × 66 Ch2 73 × 72

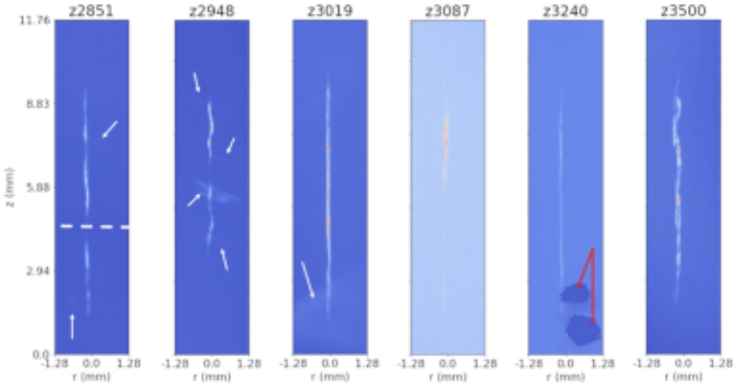

Challenges*

*By no means exhaustive

- Unspecified experiment dependent SNR
- Multiple distinct spherical crystal imaging modalities
  - Continuum vs spectral lines
  - Resolution
  - Views
- Typically no spatial fiducial
  - Registration

E.C. Harding *et. al.*, (Under Review).
W.E. Lewis *et al.,* J. Plasmas Phys. **88**, 895880501 (2022).

Several challenges make addressing these questions difficult.

Challenge

- Image metrics may vary between practitioners and studies
  - Need a framework to asses how sensitive metrics are to previous factors
  - Need statistical/larger scale studies to understand relevance to physics

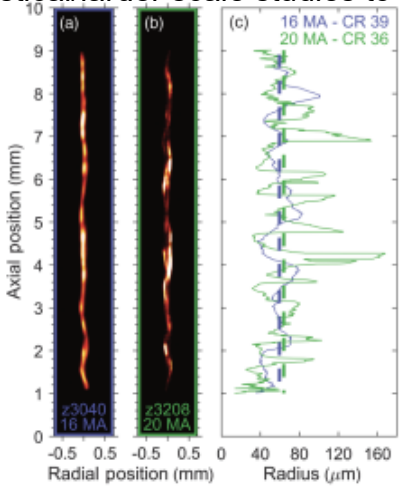

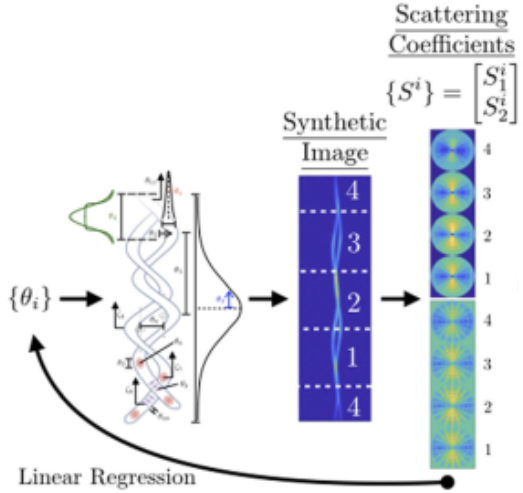

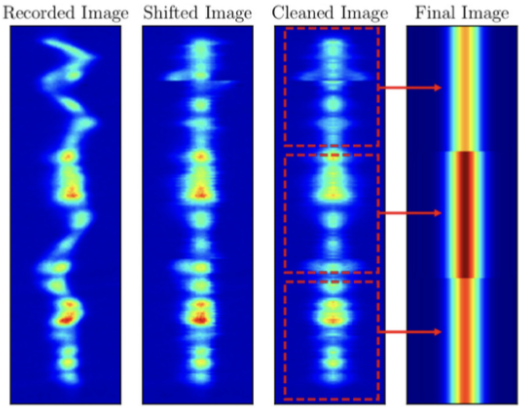

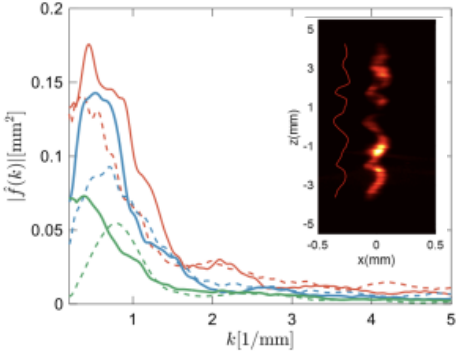

M.R. Gomez *et al.*, Phys. Rev. Lett. **125**, 155002 (2020).
M.E. Glinsky *et al.*, Phys. Plasmas **27**, 112703 (2020).
P.F. Knapp *et al.*, Phys. Plasmas **29**, 052711 (2022).
D.J. Ampleford, D.A. Yager-Elorriaga *et al.* (In Preparation).

Several challenges make addressing these questions difficult.

Challenge

- Image metrics may vary between practitioners and studies
  - Need a framework to asses how sensitive metrics are to previous factors
  - Need statistical/larger scale studies to understand relevance to physics

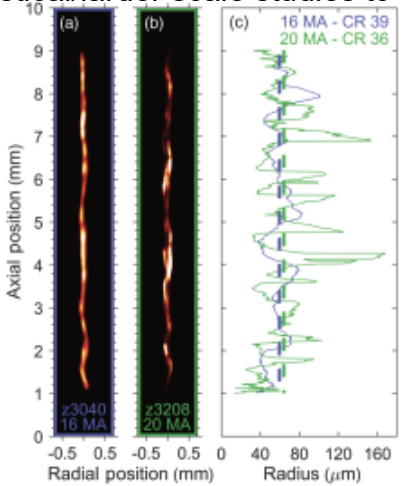

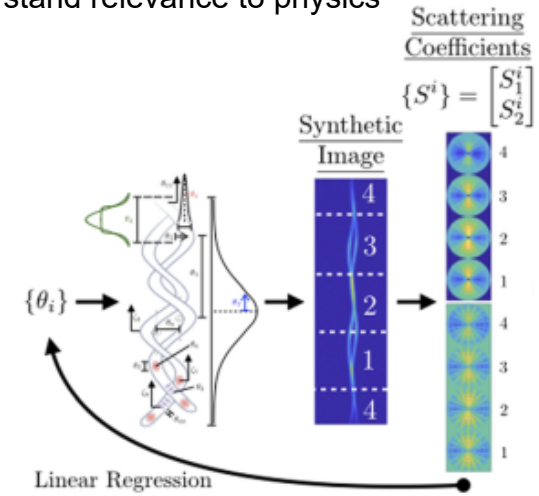

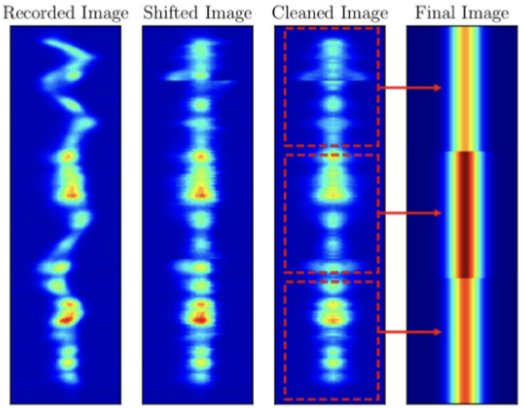

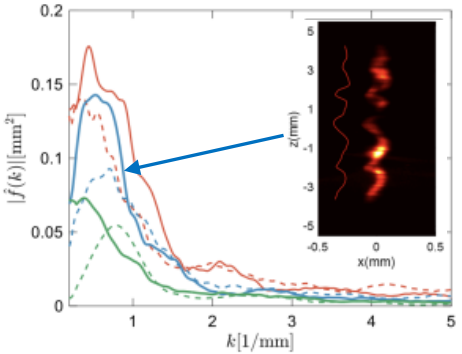

M.R. Gomez *et al.*, Phys. Rev. Lett. **125**, 155002 (2020).
M.E. Glinsky *et al.*, Phys. Plasmas **27**, 112703 (2020).
P.F. Knapp *et al.*, Phys. Plasmas **29**, 052711 (2022).
D.J. Ampleford, D.A. Yager-Elorriaga *et al.* (In Preparation).

which provides a space-scale representation amenable for image-to-image comparison.

- Band pass filtering (first order) and “cross-scale correlation” (second order)
- Scales are reasonably matched to experiment
- Stable to small deformations

$$\sin\left(k_y y + \frac{\pi}{4}\sin\left(\kappa_x x\right)\right)e^{-\frac{(x^2+y^2)}{2\sigma^2}}$$

$k_y = \frac{\pi}{8}, \kappa_x = \frac{\pi}{16}, \sigma = \frac{1}{8}$

$k_y = \frac{\pi}{4}, \kappa_x = \frac{\pi}{16}, \sigma = \frac{1}{8}$

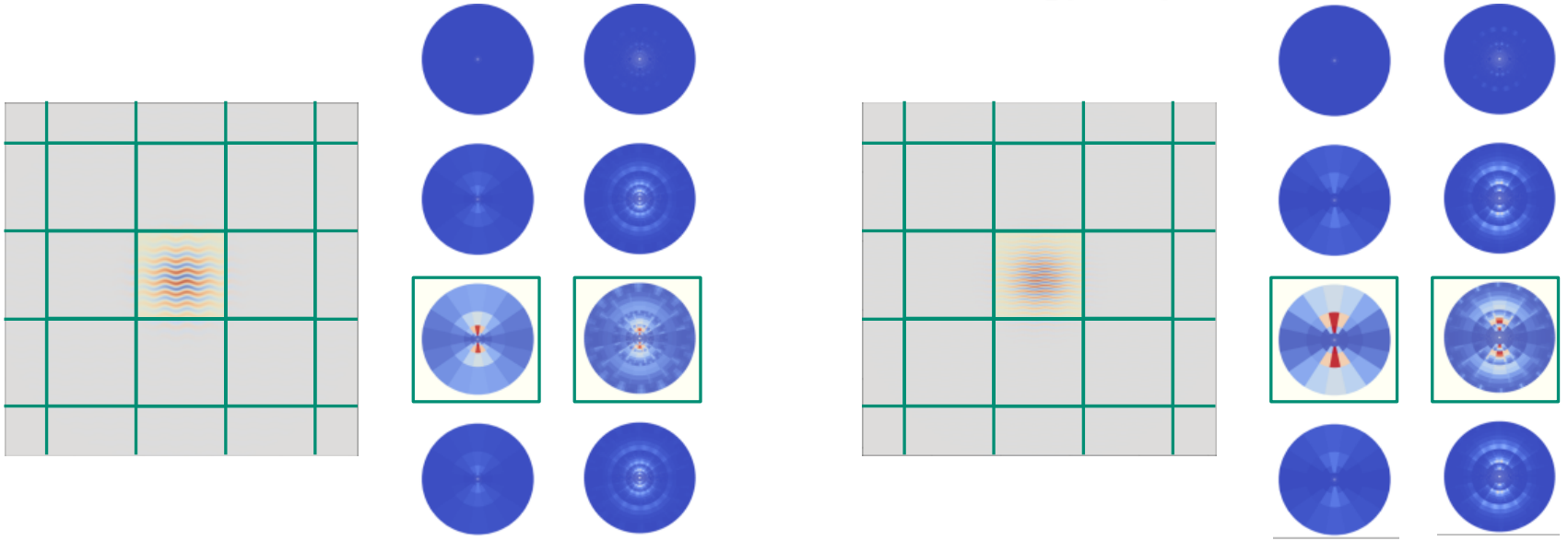

which provides a space-scale representation amenable for image-to-image comparison.

- Band pass filtering (first order) and “cross-scale correlation” (second order)
- Scales are reasonably matched to experiment
- Stable to small deformations

$$\sin\left(k_y y + \frac{\pi}{4}\sin\left(\kappa_x x\right)\right) e^{-\frac{(x^2+y^2)}{2\sigma^2}}$$

$k_y = \frac{\pi}{8}, \kappa_x = \frac{\pi}{16}, \sigma = \frac{1}{8}$

$k_y = \frac{\pi}{4}, \kappa_x = \frac{\pi}{16}, \sigma = \frac{1}{8}$

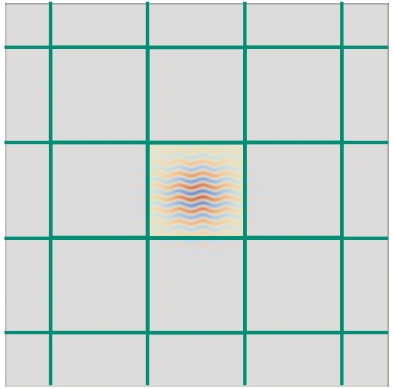

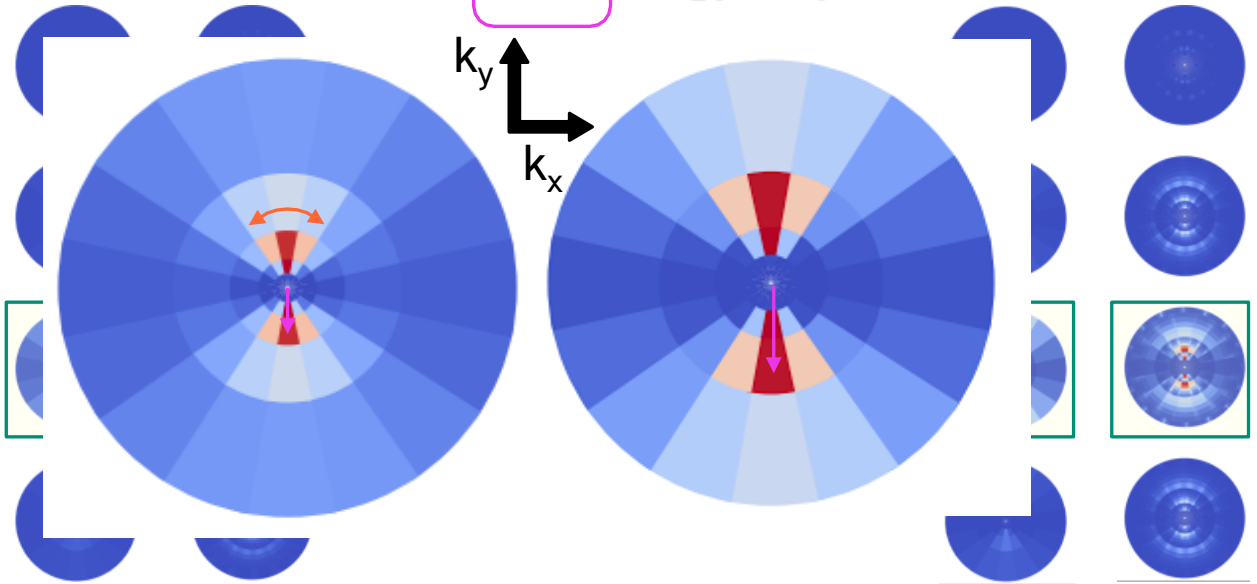

which provides a space-scale representation amenable for image-to-image comparison.

- Band pass filtering (first order) and “cross-scale correlation” (second order)
- Scales are reasonably matched to experiment
- Stable to small deformations

$$\sin\left(k_y y + \frac{\pi}{4}\sin\left(\kappa_x x\right)\right)e^{-\frac{(x^2+y^2)}{2\sigma^2}}$$

$k_y = \frac{\pi}{8}, \kappa_x = \frac{\pi}{16}, \sigma = \frac{1}{8}$

$k_y = \frac{\pi}{4}, \kappa_x = \frac{\pi}{16}, \sigma = \frac{1}{8}$

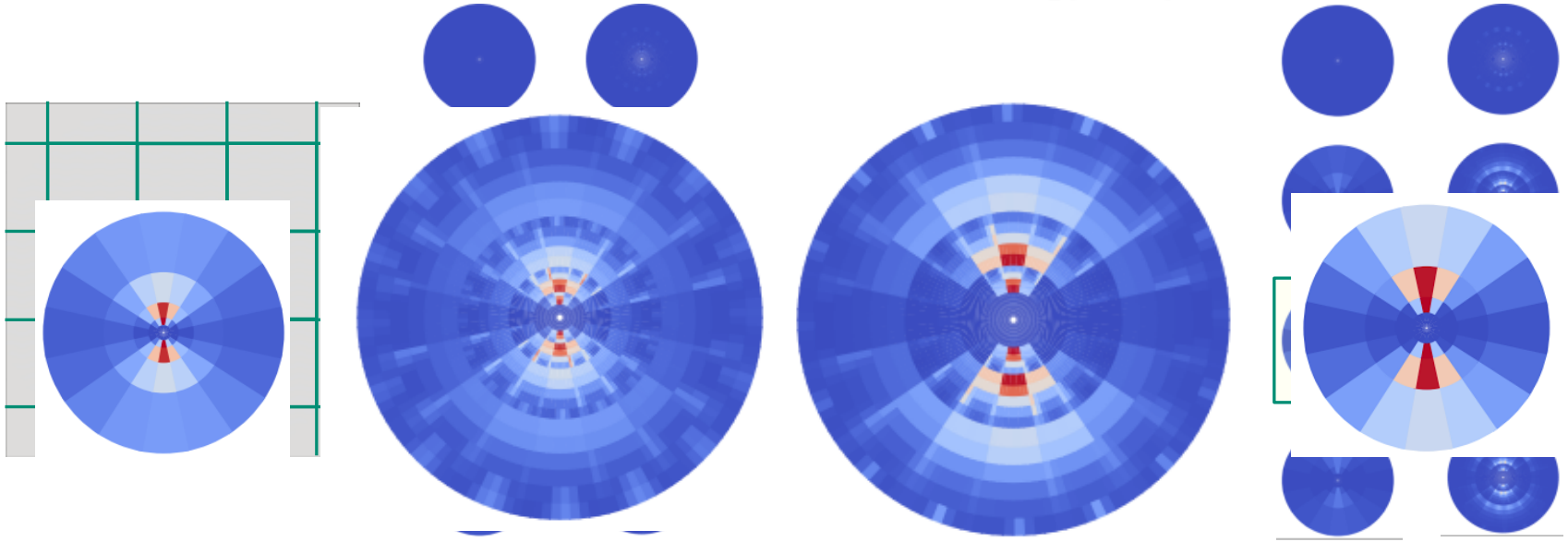

which provides a space-scale representation amenable for image-to-image comparison.

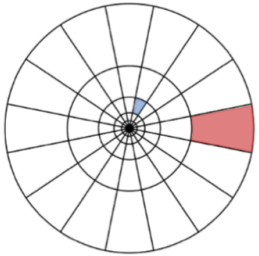

$j = 0, \ell = 0$
$j = 2, \ell = 3$

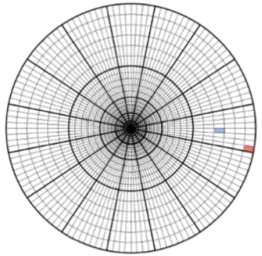

$j = 0, \ell = 0, j' = 1, \ell' = 0$
$j = 0, \ell = 0, j' = 4, \ell' = 3$

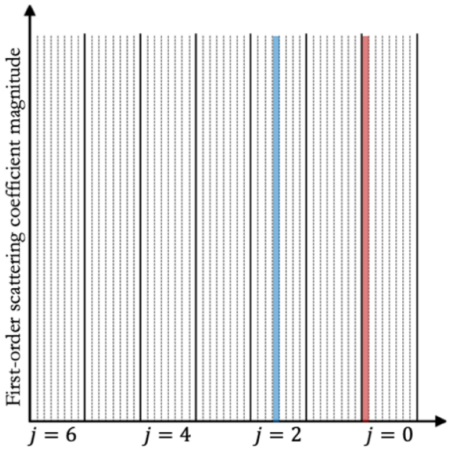

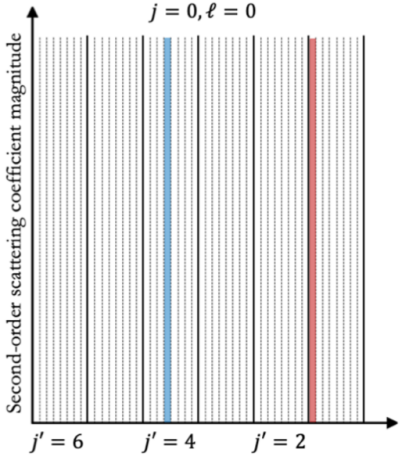

“Model-free” data augmentation can leverage known sources of variance to help understand sensitivities and engineer metrics

Sensitivity to texture/SNR via multiple scans

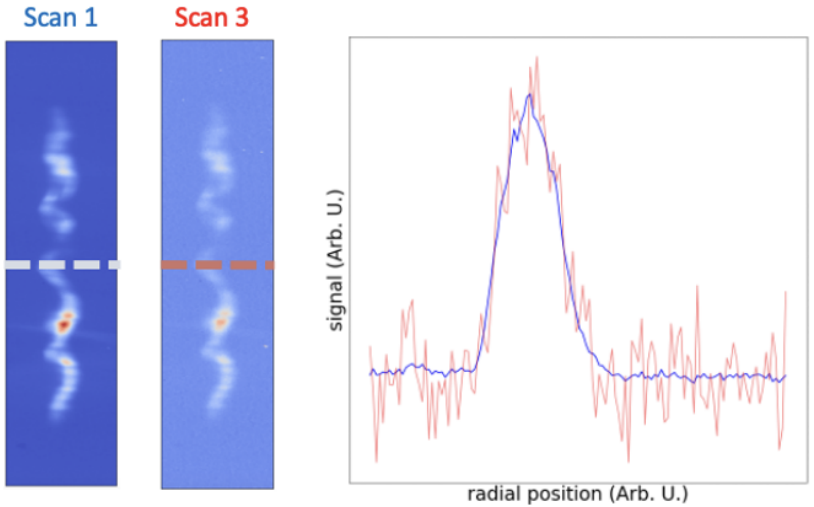

Sensitivity to resolution via PSFs and high-resolution imager data

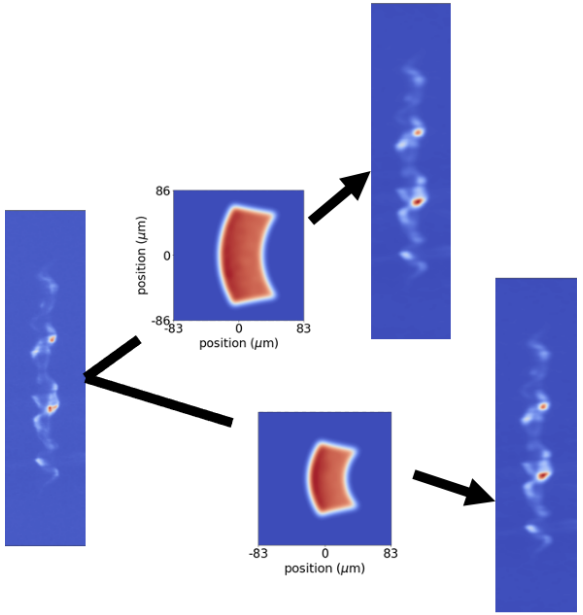

Invited paper ICDDPS-4 W.E. Lewis *et al.,* (In Preparation).

“Model-free” data augmentation can leverage known sources of variance to help understand sensitivities and engineer metrics

Sensitivity to texture/SNR via multiple scans

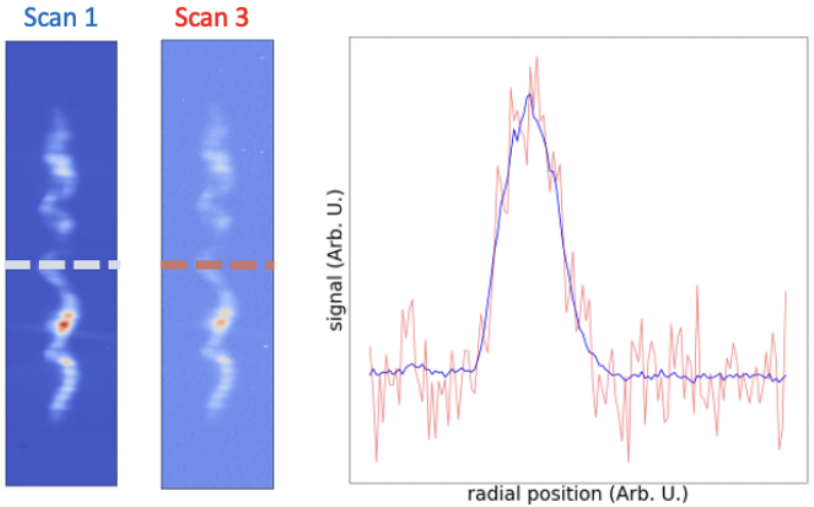

Noise filtering can remove unwanted sensitivity to SNR

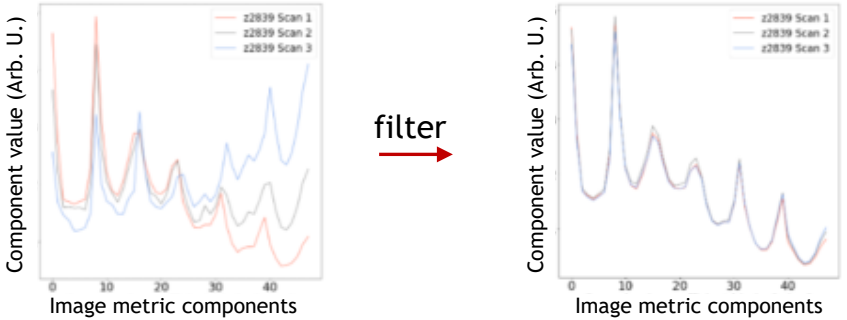

Invited paper ICDDPS-4 W.E. Lewis *et al.,* (In Preparation).

“Model-free” data augmentation can leverage known sources of variance to help understand sensitivities and engineer metrics

Sensitivity to resolution via PSFs and high-resolution imager data

Imager	Configuration	Resolution [μm^2]
High Resolution Continuum X-ray (CXI)	single	15 × 16
Dual Continuum X-ray (DCXI)	dual	Ch1 54 × 120 Ch2 46 × 84

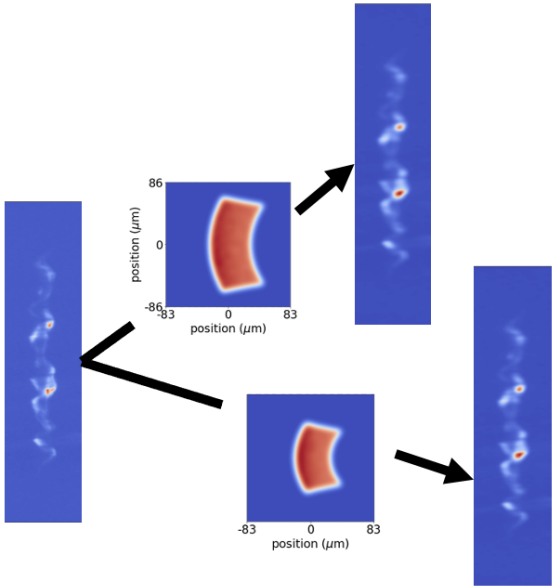

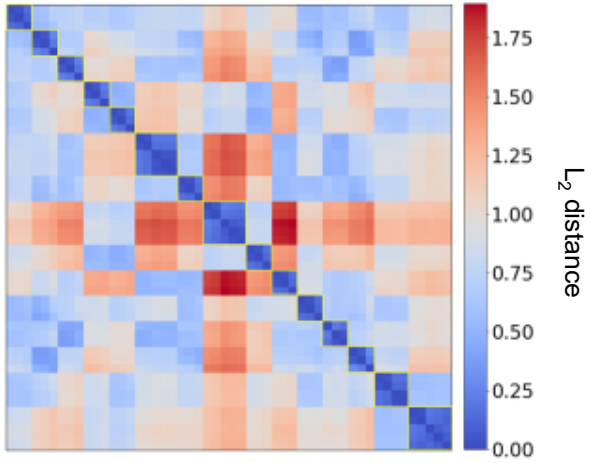

Note: Diagonal compares image to itself

= similar

= different

Nearest-neighbor identity unchanged

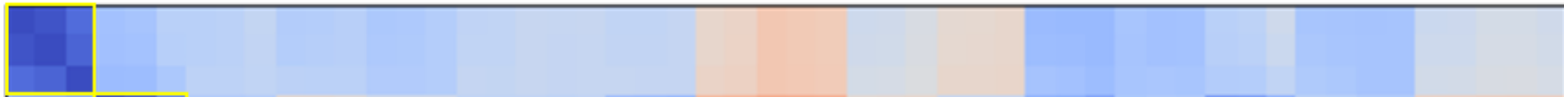

Invited paper ICDDPS-4 W.E. Lewis *et al.,* (In Preparation).

Several challenges make addressing these questions difficult.

Challenge

- Image metrics may vary between practitioners and studies
  - Need a framework to asses how sensitive metrics are to previous factors
  - Need statistical/larger scale studies to understand relevance to physics

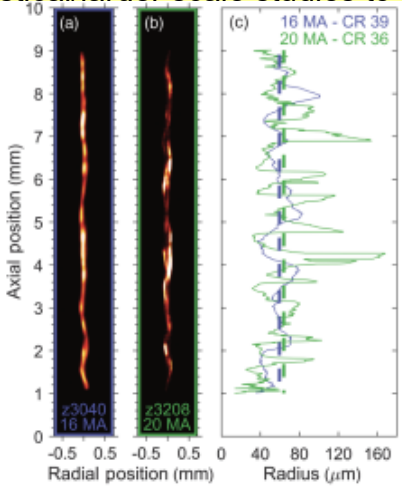

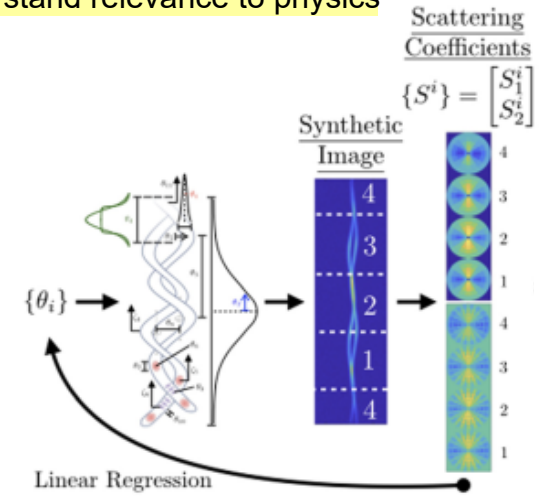

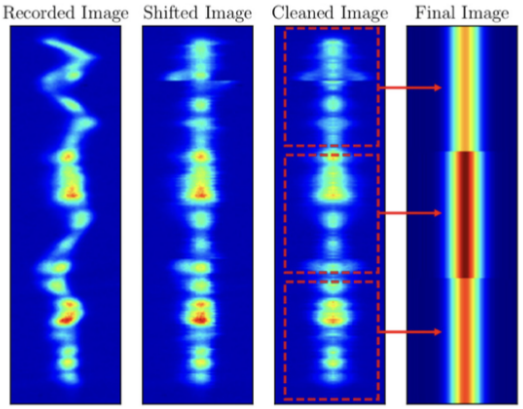

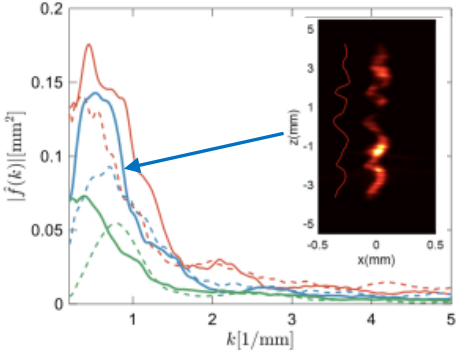

M.R. Gomez *et al.*, Phys. Rev. Lett. **125**, 155002 (2020).
M.E. Glinsky *et al.*, Phys. Plasmas **27**, 112703 (2020).
P.F. Knapp *et al.*, Phys. Plasmas **29**, 052711 (2022).
D.J. Ampleford, D.A. Yager-Elorriaga *et al.* (In Preparation).

Stagnation morphology appears to be an important piece of the puzzle of understanding performance and reproducibility

- Can we characterize relation to variance in performance?
  - 7 of top 10 performers coated

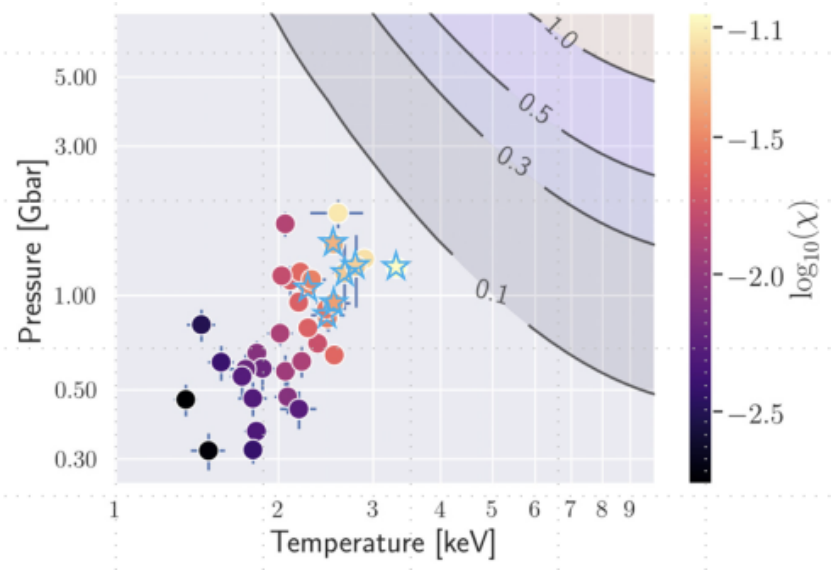

P.F. Knapp *et al.*, Phys. Plasmas **29**, 052711 (2022).

- Improved morphology/reduced mix partially r

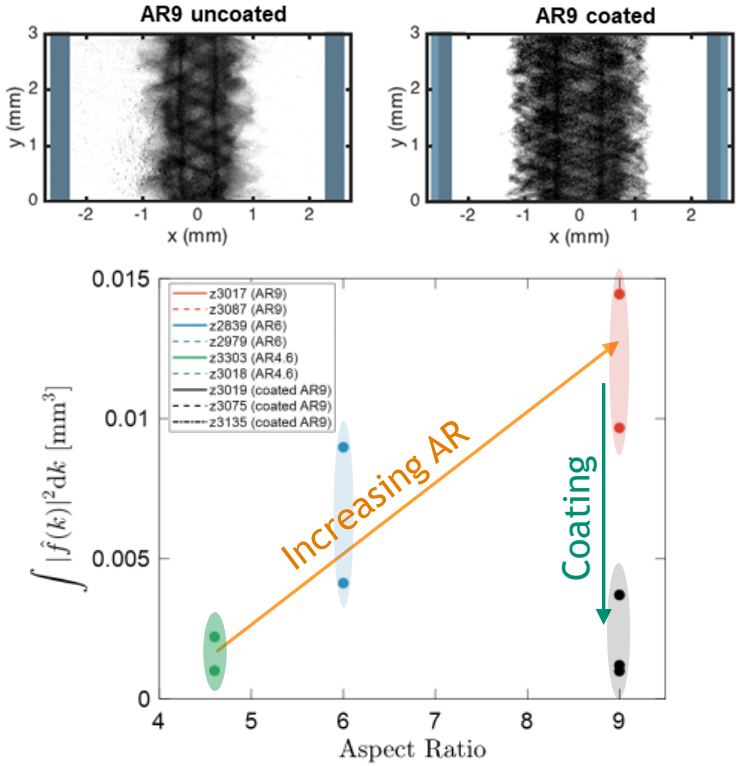

D.J. Ampleford, D.A. Yager-Elorriaga *et al.* (In Preparation).

Data-driven methods are enabling metric exploration that is building to more detailed understanding of important features.

- Stagnation images often quantified with intuitive metrics
  - **Centroid** of Gaussian fit to horizontal slices
    - Integral of the $|FFT|^2$ provides a metric for stability
- More complicated structures may be present
  - bifurcations, dim regions, *etc.*
  - may require a more advanced metrics (*e.g.* MST)

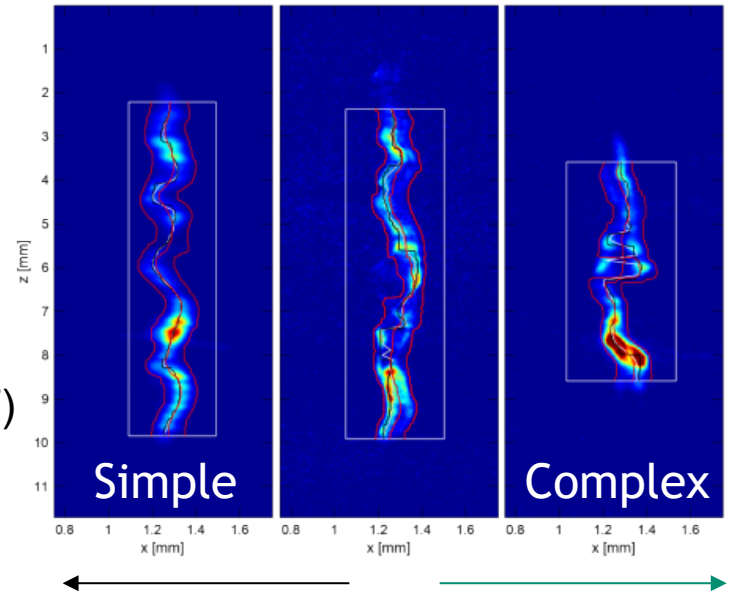

Data-driven methods are enabling metric exploration that is building to more detailed understanding of important features.

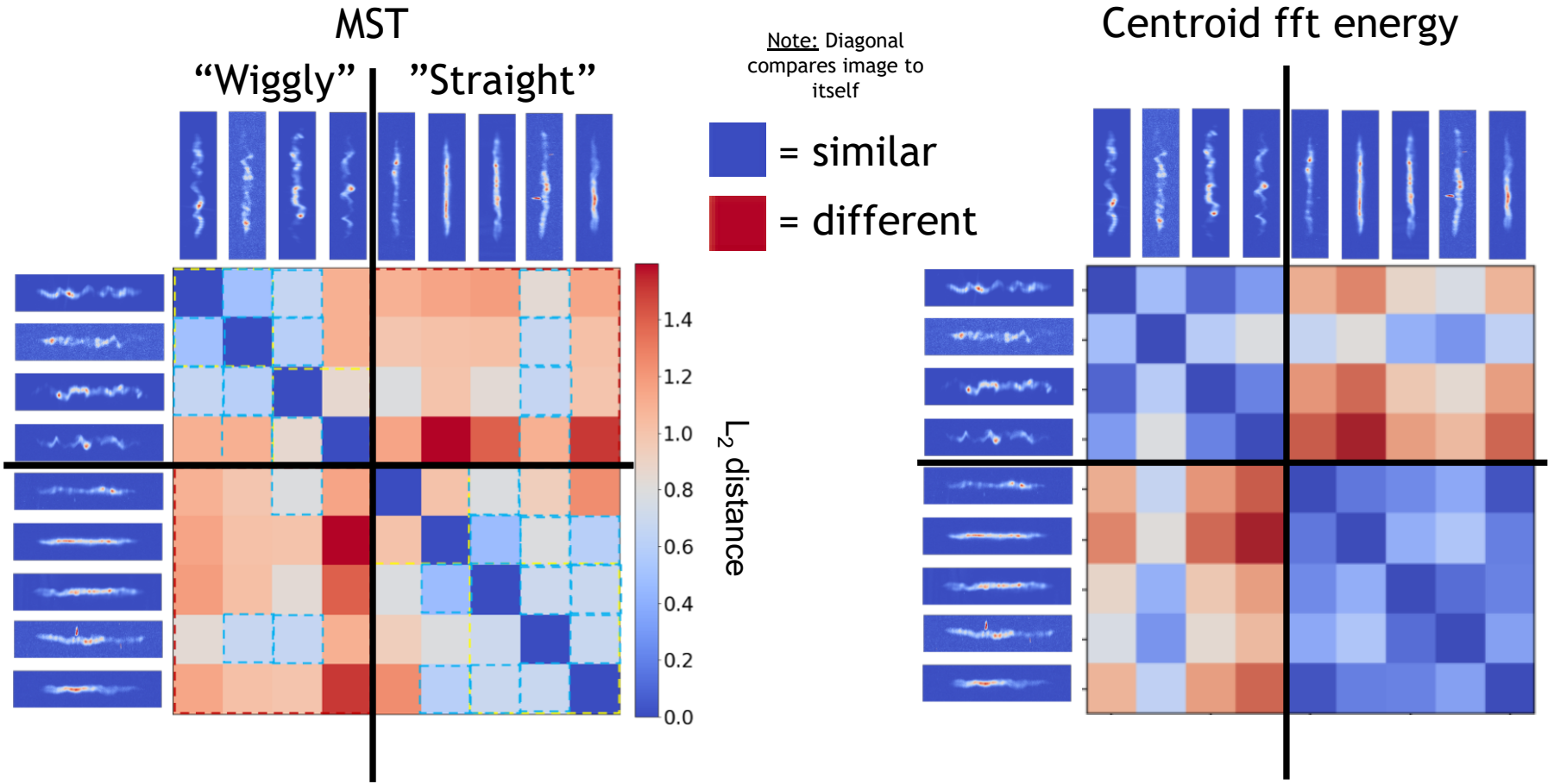

Invited paper ICDDPS-4 W.E. Lewis *et al.,* (In Preparation).

Data-driven methods are enabling metric exploration that is building to more detailed understanding of important features.

Large-scale studies can aid in investigating non-obvious structure in our data

Predicted \ True

random	u	c
$\tilde{u}$	0.74 ± 0.06	0.74 ± 0.11
$\tilde{c}$	0.26 ± 0.06	0.26 ± 0.11

MST	u	c
$\tilde{u}$	0.84	0.47
$\tilde{c}$	0.16	0.53

FFT centroid energy	u	c
$\tilde{u}$	0.64	0.08
$\tilde{c}$	0.36	0.92

*random labeling with known class imbalance ~26% coated

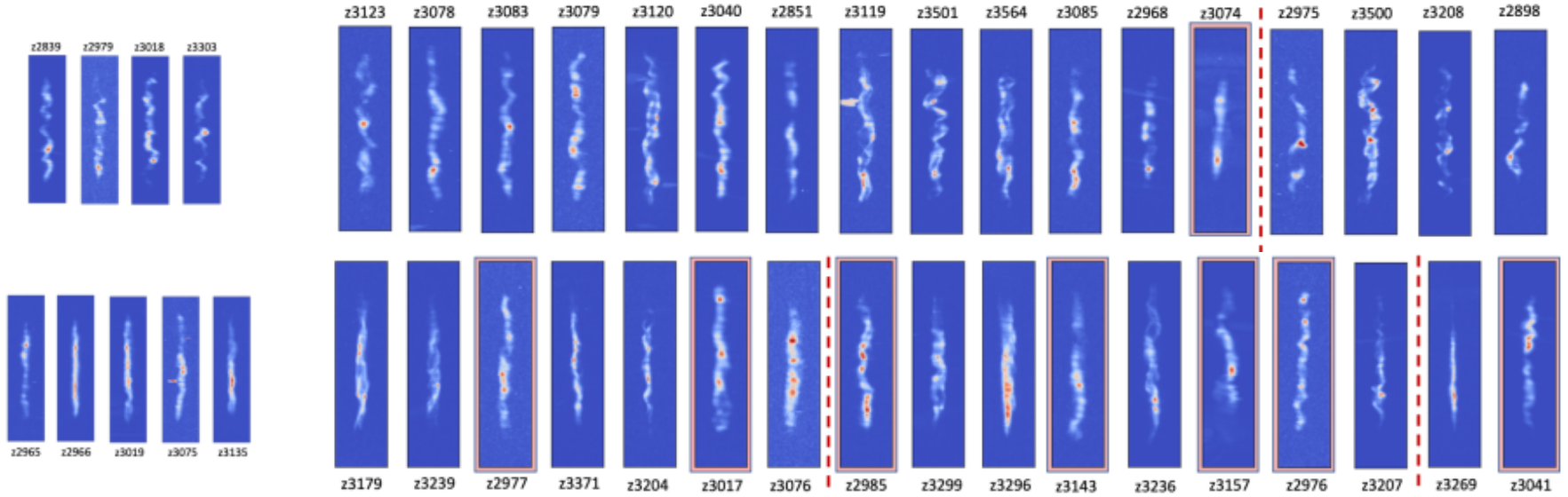

Invited paper ICDDPS-4 W.E. Lewis *et al.,* (In Preparation).

captures more information. We are investigating how to best leverage this.

FFT centroid energy	u	c
$\tilde{u}$	0.64	0.08
$\tilde{c}$	0.36	0.92

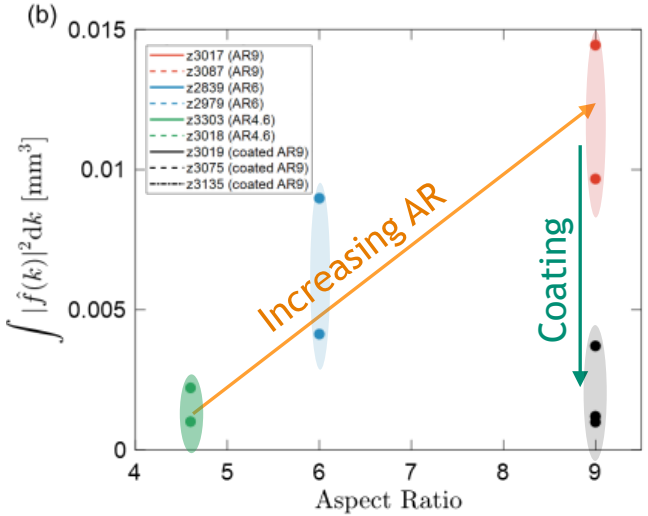

MST	u	c
$\tilde{u}$	0.84	0.47
$\tilde{c}$	0.16	0.53

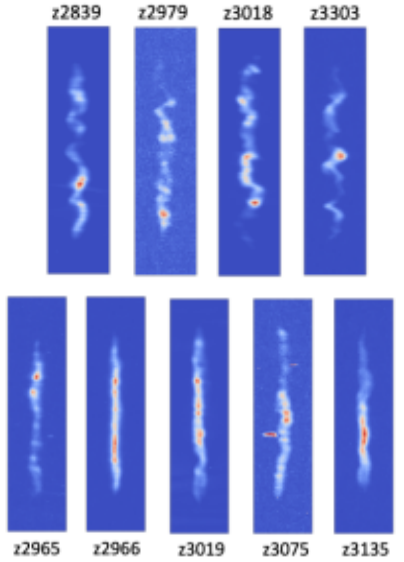

Future directions and potential for collaboration

- Extension of sensitivity study to alternate metrics

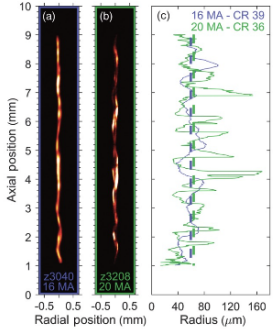

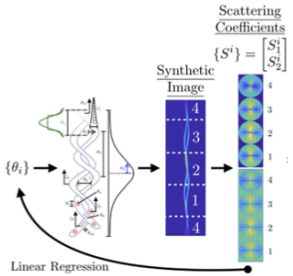

Apply model free data-augmentations and understand sensitivities

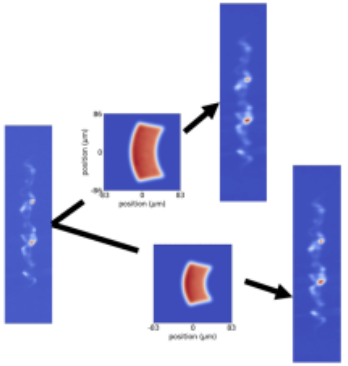

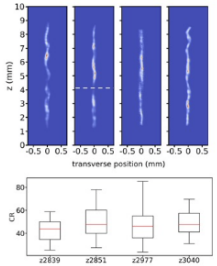

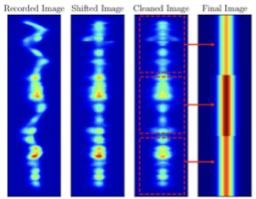

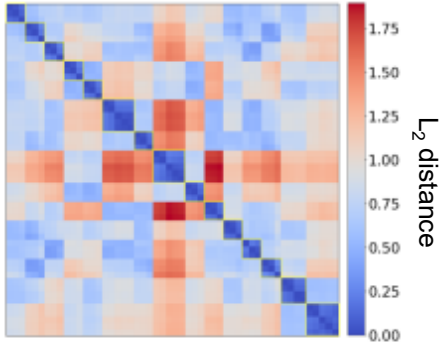

Note: Diagonal compares image to itself

= similar

= different

M.R. Gomez *et al.*, Phys. Rev. Lett. **125**, 155002 (2020).
M.E. Glinsky *et al.*, Phys. Plasmas **27**, 112703 (2020).
W.E. Lewis *et al.*, Phys. Plasmas **28**, 092701 (2021).
P.F. Knapp *et al.*, Phys. Plasmas **29**, 052711 (2022).
D.J. Ampleford, D.A. Yager-Elorriaga *et al.* (In Preparation).

Future directions and potential for collaboration

- Multiple view angles
  - Do differences in image metric between multiple views contain valuable “integrated” information?
    - E.g. value even if tomographic inversion ill-posed
- Develop metrics to quantify mix morphology, liner opacity impact, *etc.*

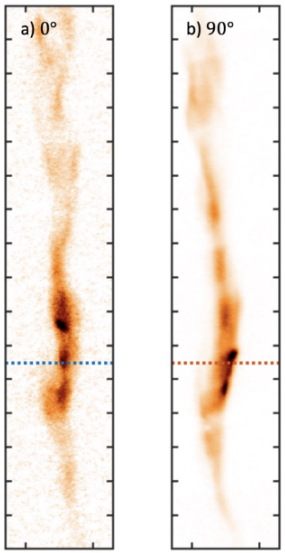

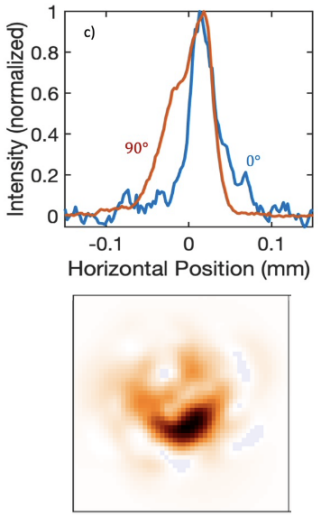

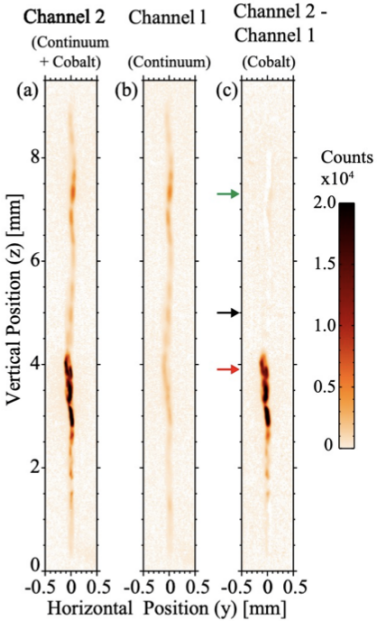

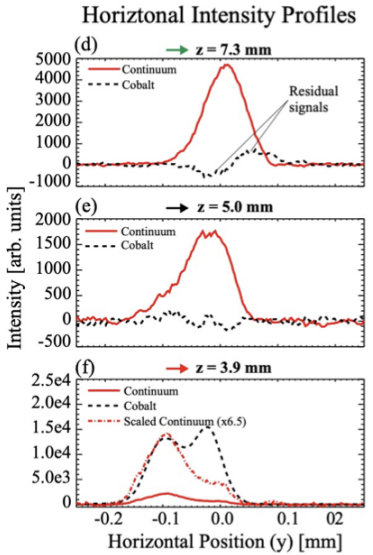

E.C. Harding *et al.* (Submitted to RSI).
J.R. Fein *et al.,* (In Preparation).

Future directions and potential for collaboration

- Applications to simulation based data to supplement insight

Helical seeds derived from experimental radiography

- 3D HYDRA simulations are initialized with a background of white noise and helical grooves
  - Defined by a depth and width
- Helices are prescribed to match previous radiographic data which indicated 7- 10 degree initialization
  - Integrated simulations use 10-20 T but lack experimental data > 10 T

Courtesy Matthew Weis

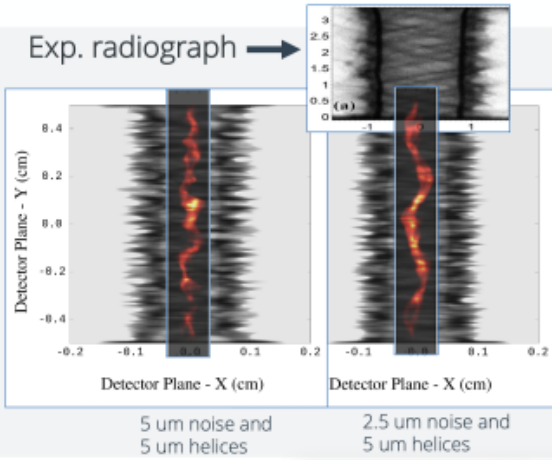

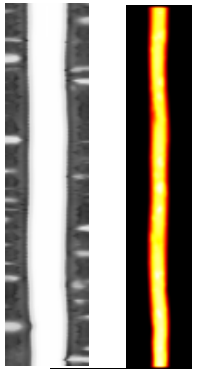

Kraken animations courtesy C.A. Jennings

Data-driven methods have found successful application across a range of problems in HEDP at Z and continues to grow!

Publications at the intersection of HEDP on Z and data science:

J. Plasma Phys. (2022), *vol.* 0. © The Author(s), 2022.
Published by Cambridge University Press
doi:10.1017/S002237782200126X

Optimizing the configuration of plasma radiation detectors in the presence of uncertain instrument response and inadequate physics

P.F. Knapp[1],†, W.E. Lewis[1], V.R. Joseph[2], C.A. Jennings[1] and M.E. Glinsky[1],‡

[1]Sandia National Laboratories, Albuquerque, NM 87185, USA
[2]Stewart School of Industrial and Systems Engineering, Georgia Institute of Technology, Atlanta, GA 30332, USA

(Received 31 May 2022; revised 29 November 2022; accepted 30 November 2022)

J. Plasma Phys. (2022), *vol.* 88, 895880501 © The Author(s), 2022.
Published by Cambridge University Press
doi:10.1017/S0022377822000800

Statistical characterization of experimental magnetized liner inertial fusion stagnation images using deep-learning-based fuel–background segmentation

William E. Lewis[1],†, Patrick F. Knapp[1], Eric C. Harding[1] and Kristian Beckwith[1]

[1]Sandia National Laboratories, Albuquerque, NM 87185, USA

(Received 5 May 2022; revised 18 August 2022; accepted 19 August 2022)

Physics of Plasmas

Estimation of stagnation performance metrics in magnetized liner inertial fusion experiments using Bayesian data assimilation

Cite as: Phys. Plasmas 29, 052711 (2022); https://doi.org/10.1063/5.0087115
Submitted: 01 February 2022 • Accepted: 01 May 2022 • Published Online: 18 May 2022

P. F. Knapp, M. E. Glinsky, M. A. Schaeuble, et al.

COLLECTIONS

Paper published as part of the special topic on Papers from the 63rd Annual Meeting of the APS Division of Plasma Physics

Physics of Plasmas

Deep-learning-enabled Bayesian inference of fuel magnetization in magnetized liner inertial fusion

Cite as: Phys. Plasmas 28, 092701 (2021); https://doi.org/10.1063/5.0056749
Submitted: 13 May 2021 • Accepted: 03 August 2021 • Published Online: 01 September 2021

William E. Lewis, Patrick F. Knapp, Stephen A. Slutz, et al.

COLLECTIONS

This paper was selected as an Editor's Pick

Journal of Applied Physics

Simultaneous inference of the compressibility and inelastic response of tantalum under extreme loading

Cite as: J. Appl. Phys. 130, 055901 (2021); https://doi.org/10.1063/5.0056437
Submitted: 10 May 2021 • Accepted: 22 July 2021 • Published Online: 05 August 2021

W. J. Schill, R. A. Austin, K. L. Schimdt, et al.

PHYSICAL REVIEW LETTERS 125, 155002 (2020)

Performance Scaling in Magnetized Liner Inertial Fusion Experiments

M. R. Gomez,[1,*] S. A. Slutz,[1] C. A. Jennings,[1] D. J. Ampleford,[1] M. R. Weis,[1] C. E. Myers,[1] D. A. Yager-Elorriaga,[1] K. D. Hahn,[2] S. B. Hansen,[1] E. C. Harding,[1] A. J. Harvey-Thompson,[1] D. C. Lamppa,[1] M. Mangan,[1] P. F. Knapp,[1] T. J. Awe,[1] G. A. Chandler,[1] G. W. Cooper,[1,3] J. R. Fein,[1] M. Geissel,[1] M. E. Glinsky,[1] W. E. Lewis,[1] C. L. Ruiz,[1] D. E. Ruiz,[1] M. E. Savage,[1] P. F. Schmit,[1] I. C. Smith,[1] J. D. Styron,[1] J. L. Porter,[1] B. Jones,[1] T. R. Mattsson,[1] K. J. Peterson,[1] G. A. Rochau,[1] and D. B. Sinars[1]

[1]*Sandia National Laboratories, Albuquerque, New Mexico 87185, USA*
[2]*Lawrence Livermore National Laboratory, Livermore, California 94550, USA*
[3]*University of New Mexico, Albuquerque, New Mexico 87131, USA*

(Received 17 January 2020; revised 31 July 2020; accepted 27 August 2020; published 9 October 2020)

Physics of Plasmas

Quantification of MagLIF morphology using the Mallat scattering transformation

Cite as: Phys. Plasmas 27, 112703 (2020); https://doi.org/10.1063/5.0010781
Submitted: 14 April 2020 • Accepted: 08 October 2020 • Published Online: 03 November 2020

Michael E. Glinsky, Thomas W. Moore, William E. Lewis, et al.

COLLECTIONS

This paper was selected as Featured

Journal of the Royal Statistical Society
Applied Statistics
Series C

Appl. Statist. (2018)
67, *Part* 4, *pp.* 1023–1045

Estimating material properties under extreme conditions by using Bayesian model calibration with functional outputs

J. L. Brown and L. B. Hund
Sandia National Laboratories, Albuquerque, USA

[Received February 2017. Final revision January 2018]

Submitted:

Data-driven assessment of magnetic charged particle confinement parameter scaling in Magnetized Liner Inertial Fusion experiments on Z

William E. Lewis,[1] Owen M. Mannion,[1] D. E. Ruiz,[1] Christopher A. Jennings,[1] Patrick F. Knapp,[1] Matthew R. Gomez,[1] Adam J. Harvey-Thompson,[1] Matthew R. Weis,[1] Stephen A. Slutz,[1] David J. Ampleford,[1] and Kristian Beckwith[1]
Sandia National Laboratories, Albuquerque, New Mexico 87185 USA

In Preparation:

A framework for experimental-data-driven assessment of Magnetized Liner Inertial Fusion stagnation image metrics

William E. Lewis,[1] Eric C. Harding,[1] Jeffrey R. Fein,[1] Patrick F. Knapp,[1] Kristian Beckwith,[1] and David J. Ampleford[1]
Sandia National Laboratories, Albuquerque, New Mexico 87185 USA

Tomographic reconstruction of MagLIF stagnation columns from orthogonal projections using learned basis functions

Jeffrey R. Fein[1] and et al.[1]
Sandia National Laboratories, Albuquerque, New Mexico 87185 USA

Data-driven methods have found successful application across a range of problems in HEDP at Z and continues to grow!

Advanced Data Analysis in Inertial Confinement Fusion and High Energy Density Physics

P. F. Knapp[1] and W. E. Lewis[1]
Sandia National Laboratories, Albuquerque, New Mexico 87185, USA

Tutorial on Bayesian inference with code

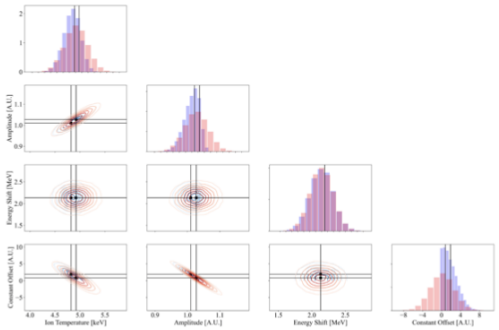

Extensive ICF/HEDP literature review of:

Bayesian inference

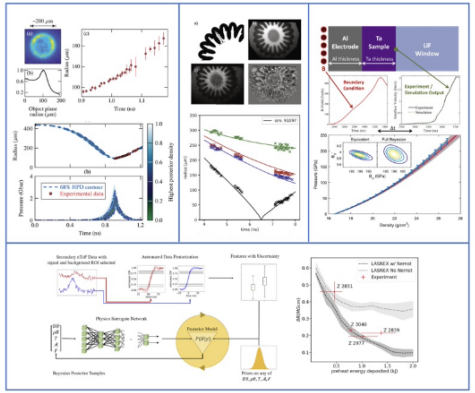

Applied ML methods

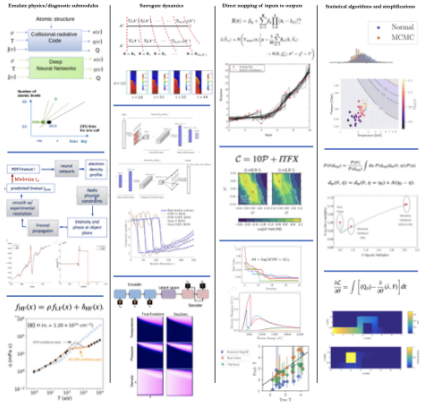

Submitted to special issue of Rev. Sci. Instrum.

Backup Slides

relation between morphology, performance, and reproducibility

- Some possible physics sources of stagnation image variance
  - preheat
    - induced mix
    - induced vorticity

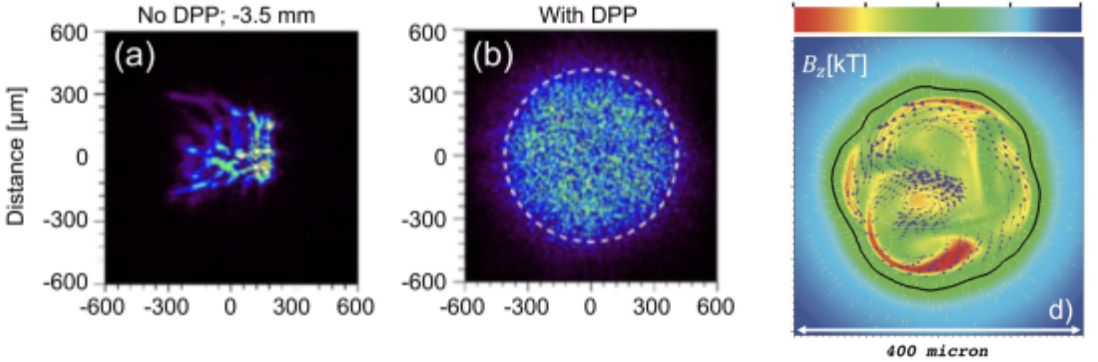

T.J. Awe *et al.* Phys. Rev. Lett. **111**, 235005 (2013).
A.J. Harvey-Thompson *et al.* Phys. Plasmas **25**, 112705 (2018).
M.R. Weis *et. al.*, Phys. Plasmas **28**, 012705 (2021).
D.A. Yager-Elorriaga *et al.* Nucl. Fusion **62**, 042015 (2022).

To understand sources of image variance we must explore experiments with targeted changes to input conditions

- Want to investigate
  - Impact of mitigation mechanisms
    - dielectric coatings
    - dynamic screw pinch
    - laser gate
    - cryogenic cooling

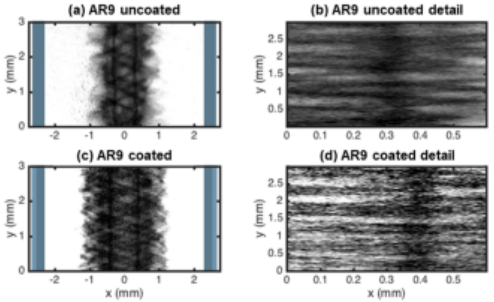

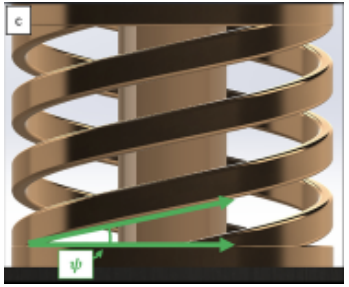

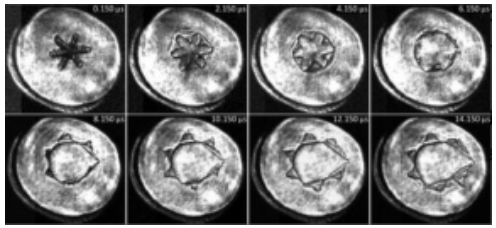

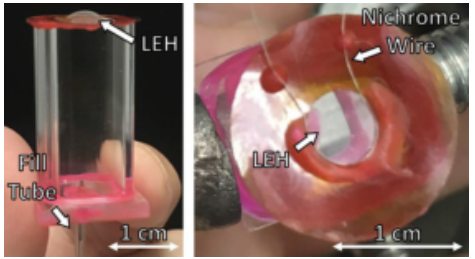

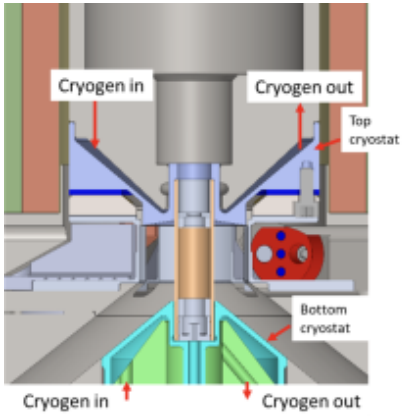

P.F. Schmit *et al.* Phys. Rev. Lett. **117**, 205001 (2016).
A.J. Harvey-Thompson *et al.* Phys. Plasmas **25**, 112705 (2018).
G.A. Shipley *et al.* Phys. Plasmas **26**, 102702 (2019).
S.M Miller *et al.* Rev. Sci. Instrum. **91**, 063507 (2020).
B.R. Galloway *et al.* Phys. Plasmas **28**, 112703 (2021).
A.J. Harvey-Thompson *et al.* Rev. Sci. Instrum. (Submitted).
D.J. Ampleford, D.A. Yager-Elorriaga *et al.* (In Preparation).

Mallat scattering transform intuition

- Band pass filtering (first order) and “cross-scale correlation/interference” (second order)
- .Nice properties, scales are reasonably matched to experiment give resolution values in each direction
- Small deformations don’t move significant signal between bands so that small changes in imager resolution etc. not expected to be critically important (but may still be present)

$$\psi(\mathbf{x}) = A(e^{i\mathbf{k}_0\cdot\mathbf{x}} - B)e^{\frac{-\mathbf{x}^2}{2\sigma_0^2}}$$

$$\psi_j^\ell(\mathbf{x}) = 2^{-j}\psi(2^{-j}r_\ell\mathbf{x}).$$

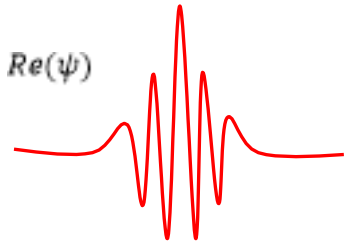

$$S_{j,\ell}^1(\mathbf{x}) = |\mathcal{I}(\mathbf{x}) \star \psi_j^\ell(\mathbf{x})| \star \phi_J(\mathbf{x}).$$

This is just a local estimate for the energy in a spectral band (j,l) at location x. I.e. a localized FFT or band-passed image.

This is a smoothing/pooling function which makes us less sensitive to e.g. translation etc.

$$S_{j,\ell,j',\ell'}^2(\mathbf{x}) = \big||\mathcal{I}(\mathbf{x}) \star \psi_j^\ell(\mathbf{x})| \star \psi_{j'}^{\ell'}(\mathbf{x})\big| \star \phi_J(\mathbf{x}).$$

Mallat scattering transform intuition (pooling of information)

- Convolution with large-scale envelop (aka father wavelet) introduces correlation, so we can safely subsample
  - Space-scale representation

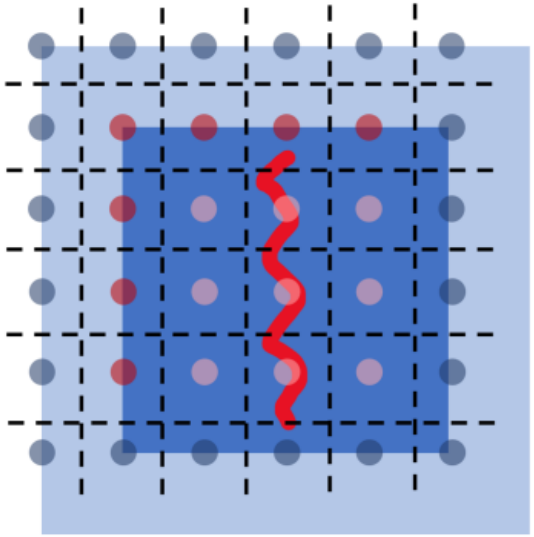

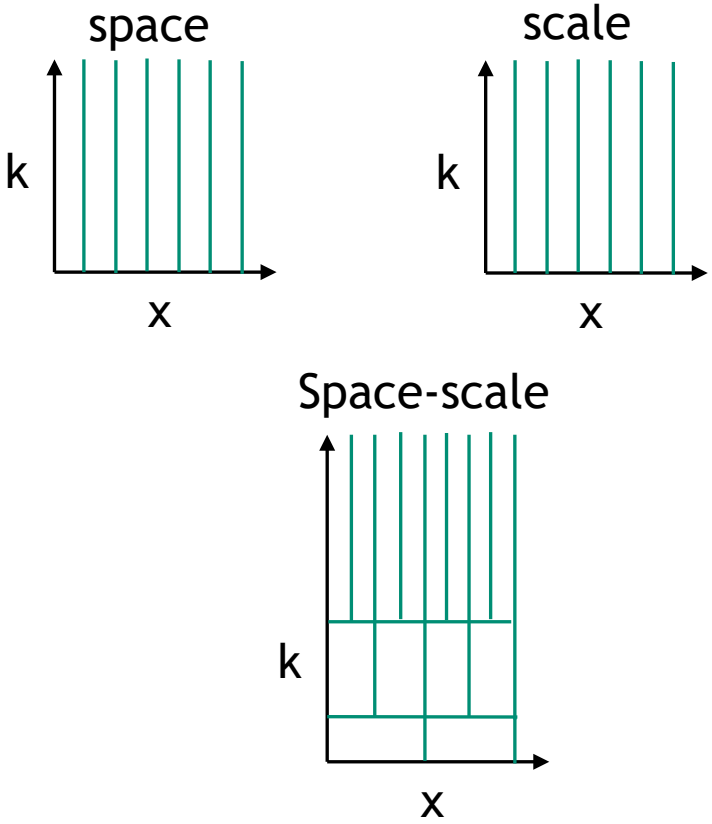

Mallat scattering transform intuition

- Band pass filtering (first order) and “cross-scale correlation” (second order)
- .Nice properties, scales are reasonably matched to experiment give resolution values in each direction
- Small deformations don’t move significant signal between bands so that small changes in imager resolution etc. not expected to be critically important (but may still be present)

```
for i in range(512):

    for j in range(512):

        tcsrc[i,j] = (np.sin(64/512*np.pi*i + np.pi/4*np.sin(32/512*np.pi*j))
                     )*np.exp((-((i-256)/512)**2-((j-256)/512)**2)/(2*(32/512)**2))
```

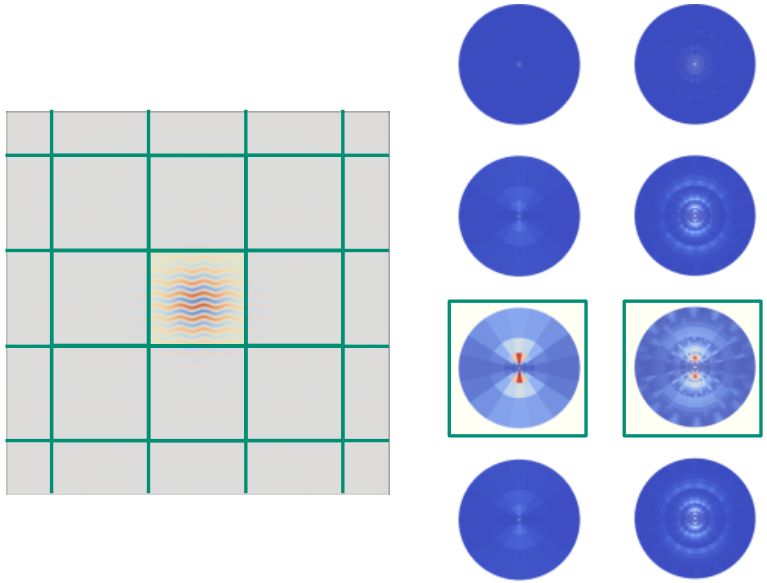

```
for i in range(512):

    for j in range(512):

        tcsrc[i,j] = (np.sin(128/512*np.pi*i + np.pi/4*np.sin(32/512*np.pi*j))
                     )*np.exp((-((i-256)/512)**2-((j-256)/512)**2)/(2*(32/512)**2))
```

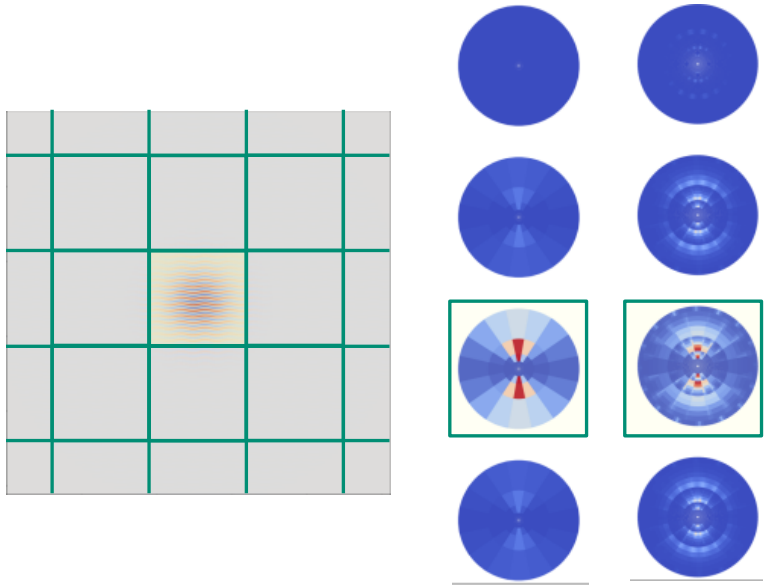

Mallat scattering transform intuition (second order)

- Convolution with large-scale envelop (aka father wavelet) reduces sensitivity e.g. to translations, but at the cost of loss of information about local coherence between frequencies.

```
y = (np.cos(1.1*np.pi*x)+np.cos(0.9*np.pi*x)+np.cos(5.7*np.pi*x+1.0)+
     np.cos(np.pi/3+1.3*np.pi*x))
```

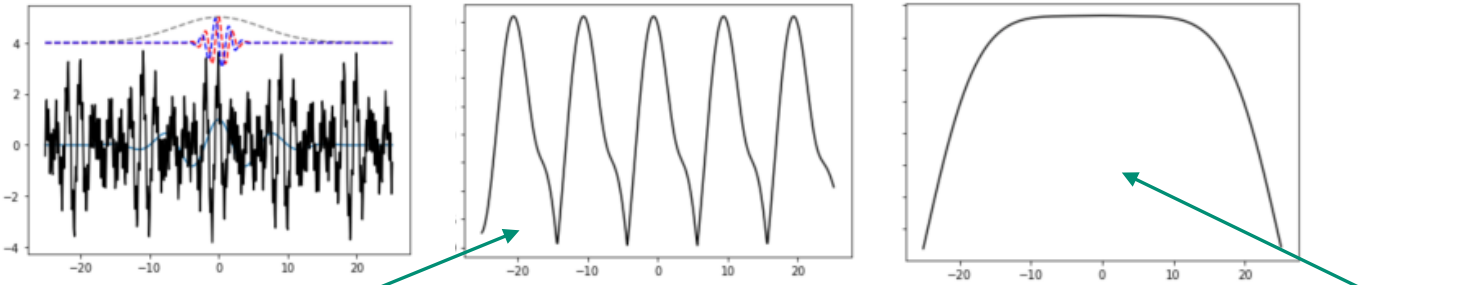

Manifestation of beat frequencies due to coherence between spectral components

$$S^2_{j,\ell,j',\ell'}(\mathbf{x}) = \big||\mathcal{I}(\mathbf{x}) \star \psi^{\ell}_{j}(\mathbf{x})| \star \psi^{\ell'}_{j'}(\mathbf{x})\big| \star \phi_J(\mathbf{x})$$

Recover coherence information by bandpass filtering again! This is basically the same info as a Fourier transform, just processed in a way to provide local spectral information.

Smoothed by convolution with father wavelet

MST visualization methods

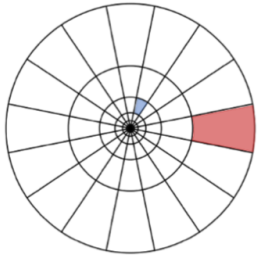

$j = 0, \ell = 0$
$j = 2, \ell = 3$

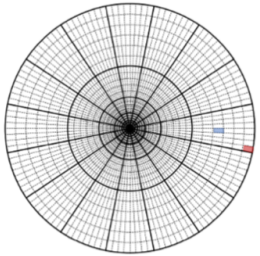

$j = 0, \ell = 0, j' = 1, \ell' = 0$
$j = 0, \ell = 0, j' = 4, \ell' = 3$